Forord

Denne master oppgaven har blitt utført ved universitetet for miljø og biovitenskap ved institutt for kjemi, bioteknologi og matvitenskap. Studien har vært en del av og blitt utført ved Protein engineering and proteimics (PEP) gruppen.

Jeg ønsker å takke alle som har hjulpet meg gjennom denne oppgaven, og da må en stor takk rettes til de flotte medlemmene av PEP gruppa som det har vært så hyggelig å bli kjent med. En spesiell stor takk til hovedveileder Vincent Eijsink og veileder Sigrid Gåseidnes som jeg har lært så utrolig mye av.

Tilslutt må jeg rette en stor takk til familien, samboer og venner: Dere har vært like fantastiske som alltid!

Tom

Abstract

This thesis describes the results of studies on the functionality and stability of CBM33 proteins. These proteins were originally defined as "Carbohydrate-Binding Modules", but it has recently been discovered that CBM33 proteins in fact are enzymes capable of cleaving polysaccharides using a combination of oxidation and hydrolysis. Some CBM33s work on chitin (Vaaje-Kolstad et al., 2005a,b, 2010), whereas others work on cellulose (Forsberg et al., 2011). The CBM33 proteins act synergistically with classical hydrolytic enzymes (i.e. chitinases, cellulases) and their use may speed up enzymatic degradation processes. Since these enzymes may be exploited for more efficient enzymatic conversion of recalcitrant biomass, they are of great scientific and commercial interest. Here we studied the CBM33 proteins CBP21, from the soil bacterium *S.marcescens* and EfCBM33 produced by *Enterococcus faecalis* a natural inhabitant of the mammalian gastrointestinal track and an opportunistic bacterium frequently often seen in hospital infections.

CBP21 acts on the insoluble polysaccharide β- chitin, one of the most widespread polymers in the world. In this study we have first tried to develop a novel method to see how effective CBP21 can bind β-chitin. The goal was to develop a more efficient assay by online monitoring of fluorescence signals as the enzyme binds to the β-chitin. The idea was then to use this assay to see whether this enzyme could bind more efficiently by adding compounds such as metals and reductants. Unfortunately, this method did not work as planned. Signals were unstable and not reproducible, and control reactions (i.e. with the enzyme but without the substrate) showed a similar decline in the signal over time as the sample with substrate. Therefore, this method was rejected.

CBP21 and EfCBM33 are very similar chitin-active enzymes, with similar functions; their 3D structures are almost identical. This was exploited in a comparative study to compare the stability of EfCBM33 relative to CBP21. CBP21 has two disulphide bridges while EfCBM33 has none, which could indicate stability differences. Unfolding assay were developed using both circular dichroism (CD) and fluorescence and by varying parameters such as the protein concentration and the heating rates. CD turned out not to be an optimal tool in measuring unfolding of CBP21 and EfCBM33 and was not routinely used in this study. The CD experiments did indicate approximately similar stabilities for the two wild-type enzymes. Measurements of intrinsic fluorescence upon a temperature increase from 20 to 80 °C yielded good apparent unfolding curves. The results did not show large differences in protein stability between the two enzymes, the difference in apparent melting temperature being

less than 2°C. DTT decreased CBP21 stability by 6.2 °C and EfCBM33 stability by only 1.5 °C, indicating that the disulfide bridges do contribute to CBP21 stability. Apparently, EfCBM33 contains other stabilizing interactions that compensate for the lacking two disulfide bonds. Of different bivalent metal ions tested, zinc ions induced a marked change in the unfolding curve, however without giving a clear change in the apparent melting temperature. This shows that metal ions do affect CBP21 unfolding behavior, but how exactly remains to be studied. It is known that divalent metals very important for enzyme activity.

In the final part of the study, attempts were made to create more stabile CBP21 variants by introducing designed single site entropic mutations that are thought to make the enzyme structure more rigid. Of three designed entropic mutations, G73A, A130P and A155P led to a 2.2 increase in the apparent Tm. CBP21 A130P is the first ever reported thermo-stabile mutant of CBM33.

Sammendrag

Denne masteroppgaven beskriver funksjonen og stabiliteten til CBM33 proteiner. Tidligere ble disse proteinene definert som ”Karbohydrat Bindende moduler” eller “Carbohydrate-Binding Modules”, men disse modulene har vist seg også å ha en enzymatisk funksjon som oksidere og hydrolysere polysakkarider. Noen av CBM33 modulene bryter ned chitin (Vaaje-Kolstad et al., 2005a,b, 2010), mens andre bryter ned cellulose(Forsberg et al., 2011). CBM33 proteinene samarbeider synergistisk med klassiske hydrolaser (for eksempel chitinaser eller cellulaser) og deres bidrag kan øke den enzymatiske nedbrytningsprosessen. Disse enzymene er av stor forskningsmessig og kommersiell interesse, siden de kan utnyttes til å gi en mer effektiv omdanning av uløselig biomasse. I denne oppgaven har vi studert CBM33 proteinene CBP21 fra jordbakterien *Serratia marcescenc* og EfCBM33 produsert av *Enterococcus faecalis*, en opportunistisk bakterie fra tarmfloraen som ofte blir sett i sammenheng med sykehusinfeksjoner.

CBP 21 er med på å bryte ned det uløselige polysakkaridet β-kitin som er en av de mest utbredte polymerene i verden. I denne oppgaven har vi først forsøkt å utvikle en ny metode for å se hvor effektivt CBP21 kan binde β-kitinet. Målet var å utvikle en mer effektiv analysering av bindingen, ved å overvåke fluorescens signalet over tid mens CBP21 bandt til β-kitinet. Deretter var tanken å bruke denne analysemetoden for å se om enzymet kunne binde mer effektivt ved tilsetning av forbindelser som metaller og reduktanter. Dessverre fungerte ikke denne metoden som planlagt da signalene var meget ustabile og heller ikke reproduserbare, mens kontrollreaksjonene (dvs. med enzym men uten substrat) viste en tilsvarende nedgang i signal over tid lik prøver med substrat. På grunn av dette ble metoden forkastet.

CBP21 og EfCBM33 er begge aktive på kitin, svært like i struktur og funksjon og deres 3D-strukturer er nesten identiske. Dette ble utnyttet i en studie for å sammenlikne stabiliteten til EfCBM33 i forhold til CBP21. CBP21 har to disulfidbroer, mens EfCBM33 har ingen. Dette kan være en indikasjon på forskjeller i stabiliteten. En denaturerings metode ble utviklet ved hjelp av sirkulær dikroisme(SD) og fluorescens der parametere som protein konsentrasjon og oppvarmings hastigheter ble variert. SD viste seg å være et ugunstig verktøy for å måle denatureringen av CBP21 og EfCBM33, og ble derfor ikke brukt rutinemessig i denne studien. SD eksperimentet indikerte lik stabilitet mellom de to villtype enzymene. Måling av indre fluorescens på CBP21 og EfCBM33 med en temperatur økning på 20-80 °C ga gode denaturerings kurver. Disse kurvene ble beregnet ut ifra en *tilsynelatende* protein-smeltetemperatur (apparent Tm). Den tilsynelatende smelte temperaturen mellom CBP21 og

EfCBM33 viste å ha en forskjell på 2 °C. DTT reduserte CBP21 stabiliteten med 6.2 °C og EfCBM33 stabiliteten med 1.5 °C, noe som indikerer at disulfidbroer bidrar til CBP21 sin stabilitet. Angivelig inneholder EfCBM33 andre stabiliserende interaksjoner som kompenserer for de to manglende disulfidbroene. Av de forskjellige toverdige metall ionene som ble testet var det sink ioner som viste en klar endring i den tilsynelatende smeltetemperaturen. Noe som viser at toverdige metaller påvirker CBP21s denaturerings prosess, til hvilken grad og hvordan gjenstår fremdeles å undersøke. Det er kjent at toverdige metall ioner er svært viktig for enzym aktiviteten til forskjellige enzymer.

I den siste delen av studiet, ble det forsøkt å skape en mer stabil CBP21 variant ved å introdusere konstruerte entropiske mutasjoner i aminosyre sekvensen. Denne mutasjonen var tenkt å gjøre enzym strukturen mer rigid. Av de tre mutasjonene som ble konstruert, G73A, A130P og A155P var det A130P variasjonen som ga en økning i den tilsynelatende smelte temperaturen. Denne økningen var på 2.2 °C. CBP21 A130P er den første CBM33 mutanten noen sinne som har blitt rapportert som en varmestabil mutant.

Index

1. Introduction

1.1 Carbohydrates

Carbohydrates occur in all plants and animals and are essential to life. Through photosynthesis, plants covert carbon dioxide to carbohydrates, mainly cellulose, starch and sugars(Hart et al. 2007). In other organisms carbohydrates are obtained directly through food or synthesized from other organic molecules such as amino acids, lactate, or glycerol. The simple carbohydrates, such as glucose, are the major nutrients of cells (Cooper & Hausman 2007; Hart et al. 2007).

Monosaccharides are the simplest carbohydrates. They contain three to seven carbon atoms and an aldehyde or a ketone functional group. If the monosaccharide contains an aldehyde group it is classified as an aldose and if it contains an ketone it is classified as ketose (McMurry et al. 2007). Monosaccharides exist mainly in cyclic, hemiacetal forms. Hemiacetal means that there are both alcohol (– OH) and ether (– O –) functional groups on the same carbon atom (the anomeric carbon). The cyclic, hemiacetal monosaccharide is formed by intramolecular nucleophilic addition, in which a reagent, in this case the hydroxyl group at the fourth or fifth carbon from the functional aldehyde or ketone, adds to the carbons of the double bond to give a product with a C – O single bond. When the cyclic hemiacetal is formed the ether is linked inside the cyclic structure while the alcohol group is sticking out (Hart et al. 2007).

The configuration of the monosaccharide is either α or β, depending on the position of the hydroxyl group at the anomeric carbon. The anomeric carbon is attached to four different groups and forms a new chiral center. The hydroxyl group is “up” in the β anomer and “down” in α anomer(Hart et al. 2007).

Monosaccharides can undergo a variety of structural changes and chemical reactions including polymerization via the formation of glycosidic bonds. They can form disaccharide from two monosaccharides. They can also form oligosaccharides (typically 2-10 units) or polysaccharides- in which many monosaccharides combine to form long chains. The solubility of oligosaccharides and polysaccharides sugars varies a lot. Polymers such as cellulose and chitin are insoluble and may form

crystalline structures. The functional groups in polysaccharides also allow reactions with alcohols, lipids and proteins to form more complex bio-molecules(Hart et al. 2007; McMurry et al. 2007).

1.2 Chitin

Chitin is the second most abundant polysaccharide in the world, after cellulose. Like cellulose, chitin is an insoluble linear polysaccharide, but opposed to cellulose it contains nitrogen. Each year more than one billion tons chitin are produced in the biosphere (Gooday 1990). Chitin is synthesized in numerous organisms and occurs for example in the shells of crustaceans and the exoskeleton of insects and other arthropods. It is also the main structural component of most fungal cell walls (Cooper & Hausman 2007; Hart et al. 2007).

1.2.1 Structure, properties and application

Chitin is a linear polymer of β-1, 4 linked *N*-acetyl-D-glucosamine (GlcNAc) It differs from cellulose in that the hydroxyl group at C-2 of each monosaccharide is replaced by an acetylamino group, CH_3CONH – (Cooper & Hausman 2007; Hart et al. 2007). The sugar units in the chitin polymer (Figure 1.1) are rotated a 180° relative to each other making the functional and structural unit a disaccharide (Horn et al. 2006b).

Chitin occurs in two major forms characterized by the arrangement of the individual N-acetyl-glucosamine chains. α- chitin, which is the most abundant form of chitin, has chains that run anti-parallel and β-chitin has chains that run parallel. There is also a third form called γ-chitin with mixed parallel/anti-parallel chains. It has been claimed that the γ-chitin should be considered a variant of the α-family (Atkins 1985). (Table 1.1) shows some of the different biological sources α- and β-chitin are found.

Table 1.1: **Biological sources of α- and β-chitin**. These two major forms of chitin contribute to the reinforcement and strength in numerous organisms.

α-chitin	Cell walls in fungus and yeast, krill, lobster, crab tendons and shells, shrimp shells, insect cuticle
β-chitin	Squid pens, tubes synthesized by pogonophoran and vestimetiferan worms, aphrodite chaetae lorica built by some seaweeds or protozoa, monocrystaline spines excreted by the diatom *Thalassiosira fluviatilis*.

(Rinaudo 2006)

The chitin polysaccharide has a packing density estimated by crystal structure data to be 1.46 g/cm^3. This density is significantly lower than cellulose (1.62 g/cm^3) meaning that chitin in principal may be easier to degrade; because water and/or enzymes can more easily penetrate the material. Chitin is fibrous and water insoluble (Eijsink et al. 2008). It is resilient because of its mechanical and chemical strength. Because of this, one would think that chitin accumulates in the nature in general, but this is not the case. Thanks to effective decomposers that can actually break down chitin, chitin has a high decomposition rate in nature. It is of interest to use enzymes from these natural chitin degraders in the development of chitin bio-refineries, where enzymatic de-polymerization plays a key role. This will require development of effective enzyme systems. As a spin-off, more insight into the enzymatic conversion of recalcitrant biomass in general may be obtained (Eijsink et al. 2008), which will be useful for the lignocelluloses-based bio-refining industry and the production of second generation bio-fuels.

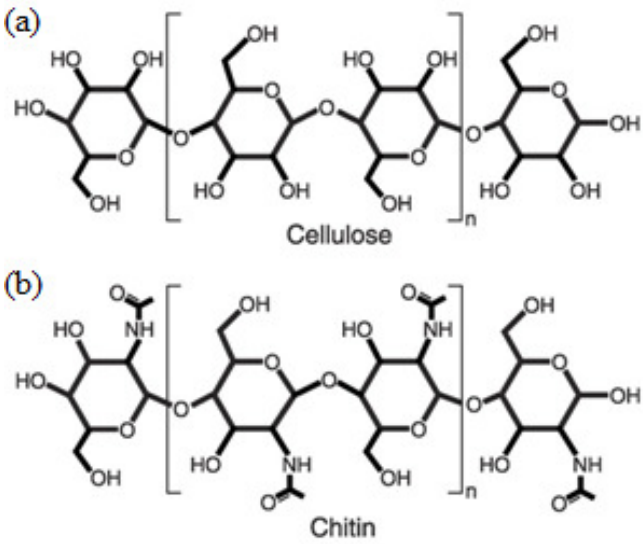

Figure 1.1: Repetitive disaccharide structures of (a) cellulose and (b) chitin (picture taken from (Vaaje-Kolstad et al. 2010)).

Since chitin is hard to degrade, its degradation usually requires the use of more than one enzyme. *Serratia marcescence* from the Enterobacteriaceae family is one of the most effective and studied chitin degrading microorganisms. When this bacterium is grown on chitin it produces three family 18 chitinases, an oxidative enzyme and a hexosaminidase (Horn et al. 2006b; Suzuki et al. 1998; Vaaje-Kolstad et al. 2005a).

1.3 Chitosan

1.3.1 Structure, properties and application

Chitosan is a derivative off chitin in which the NH_2-functional group at the C-2 position of D-glucosamine is not acetylated. Depending on the origin of the polymer, partially deacetylated chitin becomes soluble in aqueous acidic media when the deacetylation degree reaches about 50 %. The chitin molecule is then called chitosan (Rinaudo 2006).

Chitosan is unique because it is the only pseudo-natural cationic polymer. Because of this, it is able to form electrostatic complexes, with for example metals, under acidic conditions. It is soluble in acidic media and its solubility largely depends on average degree of acetylation, distribution of the acetyl groups along the main chain and molecular weight (Rinaudo 2006).

Chitosan is the most important derivative from chitin in terms of applications because it is soluble in acidic aqueous solutions. The most important applications of chitosan are in cosmetics and the pharmaceutical and biomedical applications (Rinaudo 2006), but it is also used in areas such as agriculture and water treatment (Aam et al. 2010). Some of the applications are in food industry such as thickener and clarification of fruit juices. Others are found in pharmaceutical industry in drugs, wound dressing material and bone filling material. Chitosans are non allergic, deodorizing and moisture controlling and stimulates resistance against *Escherichia coli* infection. It accelerates wound healing and suppresses the growth of tumor cells in mice (Rinaudo 2006).

1.4 Carbohydrate-active enzymes

Enzymes play a crucial role when it comes to breaking down carbohydrates, both in nature and in industry. Carbohydrate-active enzymes can change carbohydrates in four ways: Hydrolysis, transglycosylation, phosphorylation and elimination. These various reactions ways will produce different products such as new glycosides (hydrolysis and transglycosylation) , modified sugars (e.g. deacetylation, i.e. hydrolysis), sugar phosphates (phosphorylation) or unsaturated sugar products (elimination) (Withers 2010). In this thesis, the focus was on hydrolytic enzymes that degrade chitin classified as glycoside hydrolases family 18 (GH18) and on accessory enzymes classified as Carbohydrate-Binding-Modules family 33 (CBM33). In light of this, the CBM33 the enzymes Chitin Binding Protein 21 (CBP 21) from *S.marcescenc*, a CBM 33 secreted by *Enterococcus faecalis* (EfCBM33), and a family GH18 chitinase called Chitinase B (Chi-B) from *S. marcescens* are discussed in more detail.

1.5 Glycoside hydrolases

Glycoside hydrolases (GH) are sometimes referred to as glycosidases or glycosyl hydrolases. They can be classified in many different ways based on their sequence, -3D structure similarities, substrate specificity and mode of action. The so-called CaZy classification of these enzymes into different classes is used as a tool to reveal evolutionary relationship and mechanistic information (Henrissat & Romeu 1995; Henrissat & Davies 1997). The Carbohydrate Active enzymes (CaZy) database is still growing. Glycosyl hydrolases break glycosidic bonds in glycosides, glycans and glycoconjugates by hydrolysis (McMurry et al. 2007; Vuong & Wilson 2010). They can catalyze the hydrolysis of –O, –N and –S linked glycosides.

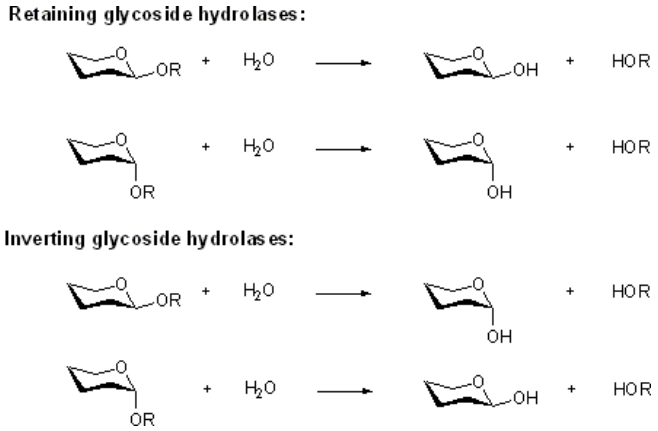

Figure 1.2: Possible outcomes of retaining and inverting mechanisms in glycoside hydrolases (picture taken from (Withers & Williams 2011)).

1.5.1 Mechanism

There are two main mechanisms in glycoside hydrolases, which either gives a net retention or inversion of the configuration of the anomeric carbon in the end substrate product (Figure 1.2). A retaining mechanism implies that the oxygen group at the anomeric carbon has the same configuration (α or β) as in the substrate. In an inverting mechanism the opposite is happening; the functional oxygen group at the anomeric carbon changes position after catalysis. The mechanisms are illustrated by (Figure 1.3)

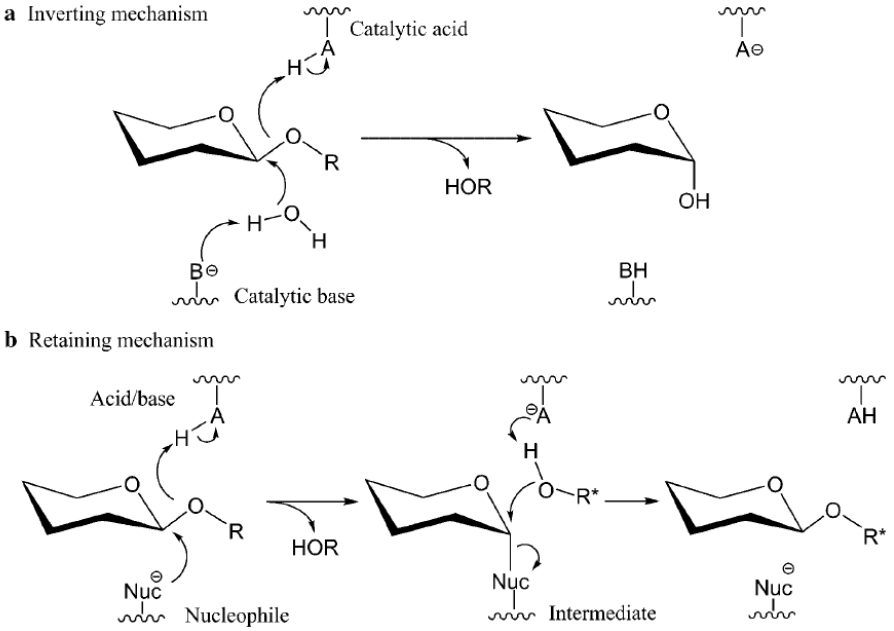

Figure 1.3: Proposed inverting (a) and retaining (b) mechanism for glycoside hydrolases. AH, catalytic residue acting as acid; B, residue acting as base; Nuc, residue acting as nucleophile; R, a carbohydrate derivative; HOR; an exogenous nucleophile, usually a watermolecule. All three residues shown (A, B & Nuc) are usually either Asp or Glu (picture taken from (Vuong & Wilson 2010)).

In the inverting mechanism, the enzyme has two catalytic residues acting as a catalytic acid- and a catalytic base. The catalytic acid donates a proton to the glycosidic bond, promoting leaving group departure, while the catalytic base makes a water molecule more nucleophilic by acting on one of the protons. Because of this, the activated water molecule has the ability to attack the anomeric center (Vuong & Wilson 2010).

In the retaining mechanism, the reaction is carried out by a general acid-base that first acts as an acid, then as a base. First, the acid donates a proton to the glycocidic oxygen. This makes the conditions right for the departure of the leaving group. At the same time, a nucleophile on the enzyme forms a covalently intermediate with the anomeric carbon. In phase two the de-protonated

acid / base functions as a base; it will de-protonate a water molecule that will carry out a nucleophilic attack on the covalent intermediate formed between the enzyme and the anomeric carbon (Vuong & Wilson 2010).

Another way to classify GHs, in addition to classifications based on sequence (CaZy) or mechanism, concerns their endo- and exo glycoside mode of action, that is how they exactly bind and catalyze the polysaccharide chains. Enzyme action can either be exo-acting or endo-acting, depending on whether the enzymes acts at chain ends or at "internal positions" on the polymer (Figure 1.4).

1.5.2 endo- and exo- acting enzymes

Enzymes that catalyzes its substrate in a randomly manner are said to be endo-acting, while exo-acting if the enzyme is reacting on chain ends(Vaaje-Kolstad et al. 2010).

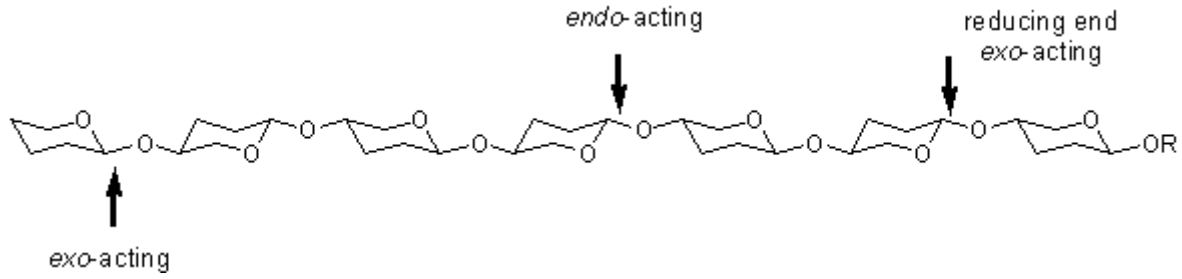

Figure 1.4: **Illustration of endo- and exo- acting enzymes**. Exo- acting enzymes often acts at the non-reducing end; these enzymes may cleave of monomers, as illustrated, but do most often produce dimers (picture taken from (Withers & Williams 2011)).

True exo-enzymes tend to have their active sites located in a pocket while true endo-enzymes tend to have their active sites located in an open cleft. For the exo-enzymes the number of sub-sites able to bind the substrate is largely dependent on the depth and shape of the active site pocket, which is also reflected in the length of the products (usually a mono- or dimeres). In the case of endo-enzymes, open catalytic clefts allow a random binding and catalysis within the polymer chain (Henrissat & Davies 1997; Proctor et al. 2005). Both these modes of action, exo- or endo-, may be combined with processivity.

1.6 Processivity

Chitin consists of crystalline and fibrous polysaccharide chains with few exposed chain ends. Some of the enzymes capable of degrading chitin have therefore developed an ability to carry out processive or multiple attack degradation. This means that the enzyme is able to perform many hydrolytic attacks without having to fully release the polysaccharide chain (Horn et al. 2006b).

Processive enzymes, for chitinases sometimes referred to as chito-biohydrolases, have active sites which are shaped like long deep clefts or tunnels. The polymeric substrates slides through and is cleaved off at the center (Eijsink et al. 2008; Rouvinen et al. 1990). Because of the periodicity in the substrate (Figure 1.1) processive enzymes usually produce dimers (Figure 1.5).

Processivity is considered advantageous for enzyme acting on crystalline polysaccharides because the polymer chain, which is bound tightly in an enzyme-substrate complex, is prevented from re-associating with the crystalline polysaccharide between each round of catalysis. Although it is not entirely clear how processivity contributes to the enzyme efficiency, there are clear experimental data showing that processivity is beneficial for chitin degradation (Horn et al. 2006a). Interestingly, in this same study, where non-processive Chi-B were generated by mutagenesis, it was shown that processivity in fact is un-favorable for degradation speed when the substrate is soluble, i.e. highly accessible (Eijsink et al. 2008).

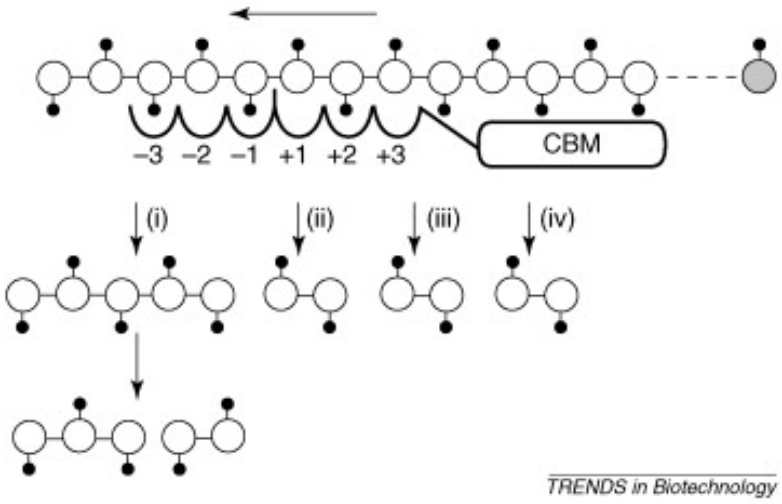

Figure 1.5: Processive degradation of chitin. The numbers (i-iv) indicate four consecutive cuts in the polymer resulting from the same initial formation of an enzyme-substrate complex. The N-acetyl groups of the chitin molecule are represented as black ball on sticks. The grey ball represents the reducing end of the sugar. The arrow indicates the direction of processivity. Apart from the first product (a pentamer in this case), all products released are dimmers (picture taken from (Eijsink et al. 2008)).

1.7 Glycoside hydrolase family 18 and Chitinase B from *Serratia marcescence*

S.marcescen secretes three chitinases- Chi A, Chi B and Chi C, that all belong to the GH18 family. The respective chitinases consist of a conserved catalytic domain and one or two, smaller domains involved in substrate binding (figure 1.6). It is important to notice how different the structure of Chi-B is compared to CBP21 (figure1.9) Chi B will be the main focus of this section, since this was the chitinase used during the laboratory work.

1.7.1 The catalytic domain

The catalytic domains in family GH18 enzymes have a $(\alpha/\beta)_8$ barrel catalytic domain with about six sugar binding sub-sites (Horn et al. 2006b; Hrmova & Fincher 2001). The $(\alpha/\beta)_8$ barrel, which is also known as the TIM barrel is a conserved protein folding pattern, consisting of eight α-helixes surrounding eight parallel β-sheets (Janecek 1993). The $(\alpha/\beta)_8$ fold is the most common enzyme fold and is shaped in such a way that parallel β-strands form a barrel in the middle of the enzyme, while the α-helices surround them. The α-helices and β-strands are connected by loops that vary in size and may even extend to complete sub-domains (as in Chi-B, Figure 1.6) (Sterner & Hocker 2005).

All GH18 contain a conserved DxxDxDxE sequence motif where x represents any residue and D and E represents aspartic acid and glutamic acid respectively. It is the glutamate in the motif that functions as the catalytic acid (Glu144 in Chi-B) (van Aalten et al. 2000).

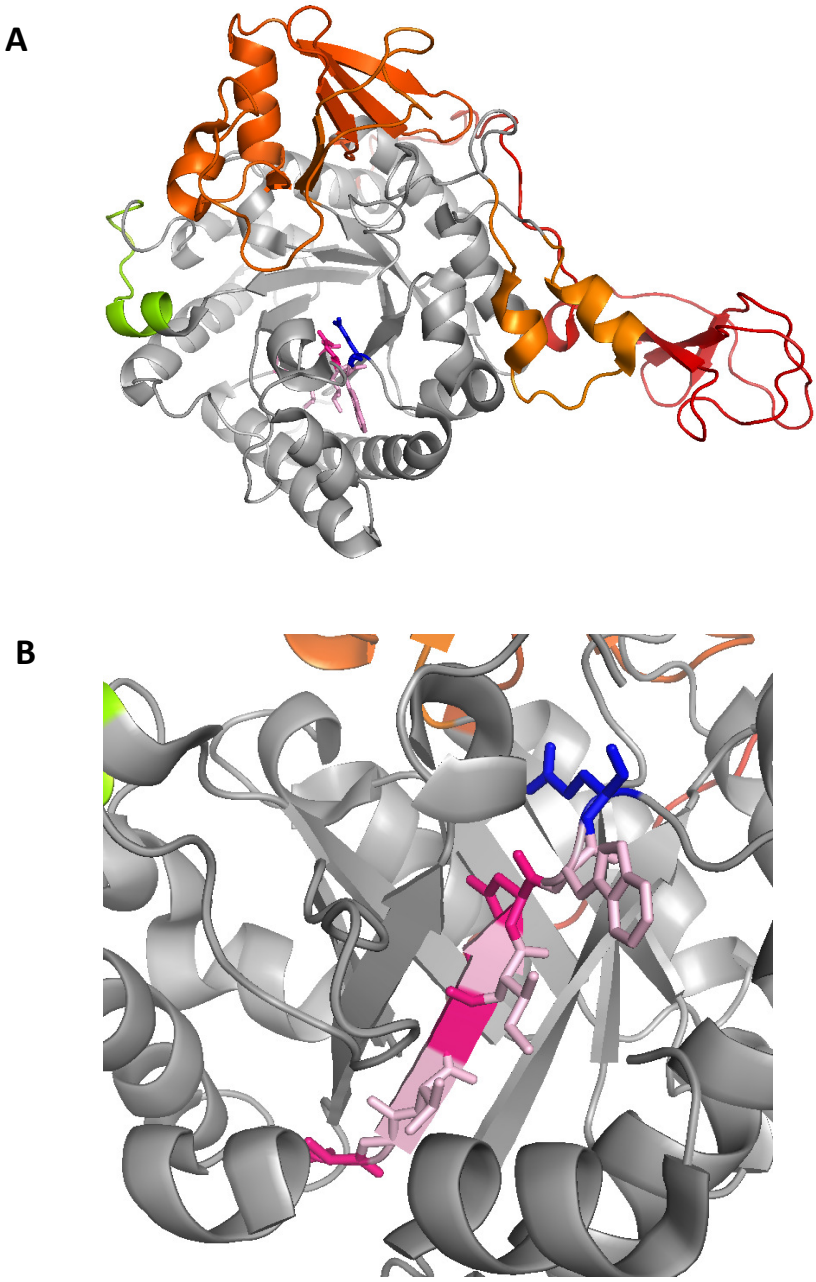

Figure 1.6: **Structure of Chi-B (PDB code 1E15)** a GH18 chitinase from *Serratia marcescenc*. The $(\alpha/\beta)_8$ barrel is shown in grey, whereas the most important insertions in the barrel have different colors. The side chains of the DxxDxDxE motif are shown in pink (non-conserved), magenta (conserved D) or blue (conserved E). The inserts shown in panel A are the "porch loop" (green) closing off the substrate-binding cleft (green; van Aalten et al., 2000), the $\alpha + \beta$ domain makes up a "wall" of the deep substrate-binding cleft (dark orange, top), and the C-terminal chitin-binding domain (dark orange, pointing to the right) and to inserted loops interacting with it (lighter orange). (van Aalten et al. 2000). The images were made with the PyMOL visualization program.

1.7.2 Catalytic mechanism

The GH18 family has a retaining mechanism and the but enzymes use a substrate-assisted double displacement reaction mechanism to carry out the acid-base reaction, where the *N*-acetyl group at the substrate acts as an intramolecular nucleophile leading to the formation of an oxazolinium ion intermediate (Synstad et al. 2004; van Aalten et al. 2001). The conserved aspartates in the DxDxE motif are involved in positioning and activating this *N*-acetyl group (Fig. 1.7). Nucleophilic attack by the *N*-acetyl group is accompanied by donation of a proton to the glycosidic oxygen by the catalytic acid. In the second step of the reaction the catalytic glutamate acts as a base and activates the water molecule that hydrolyses the oxazolinium ion intermediate (Tews et al. 1997; van Aalten et al. 2001).

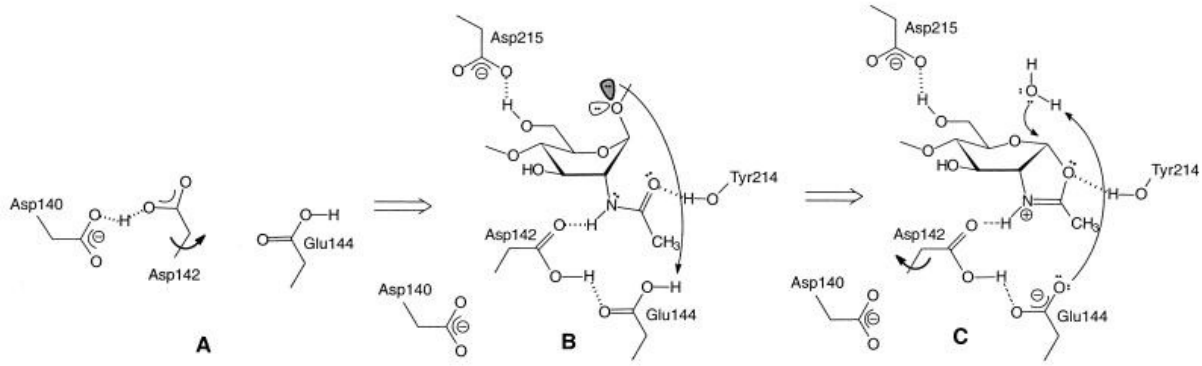

Figure 1.7: **Substrate-assisted catalysis in the GH18 family** (Synstad et al. 2004; van Aalten et al. 2001)

1.8 Carbohydrate Binding Modules

Carbohydrate binding modules (CBMs) are defined as proteins capable of binding carbohydrates. Most of them occure only as parts of an enzyme but there are rarer cases of CBMs operating alone. The large number of Carbohydrate Binding Modules discovered through genome sequencing has led to the introduction of a CBM group in the CaZy database (Davies and Henrissat 2002). The CBMs are divided into families based on similarities in their amino acid sequence (Henrissat et al. 1998). Figure 1.8 schematically illustrates how CBMs are thought to contribute to substrate binding in two chitinases.

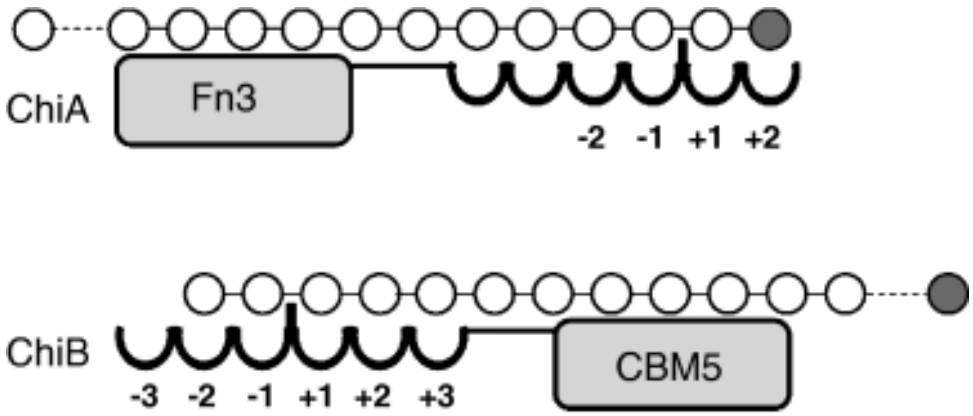

Figure 1.8: Schematic illustration of how the GH family 18 enzymes chitinase A and B from *Serratia marcescens* bind to chitin. Substrate sub-sites are marked with numbers and chitin binding domains shown as boxes. Fn3 strands for fibronectin type 3 domain a chitin-binding domain that has not yet been classified as a CBM. CBM5 stands for a carbohydrate binding module belonging to family 5. The grey ball indicates the sugar unit at the reducing end. Note that the substrates in these two processive *S. marcescens* enzymes are orientated in opposite directions. This picture was taken from Horn et al. 2006b.

The CBMs were originally thought to bind cellulose, but their preferences for binding ligands turned out to be more diverse. Carbohydrates for which specific CBMs have been described include crystalline cellulose, non-crystalline cellulose, chitin, *β*-1,3-glucans , *β*-1,3-1,4-mixed linkage glucans , xylan, mannan, galactan and starch (Boraston et al. 2004). Interestingly, as discussed elsewhere in this thesis, CBMs in family 33 seem to be erroneously classified as CBMs since these proteins in fact are enzymes (Vaaje-Kolstad et al., 2010). CBM33 domains most often occur in proteins lacking any other enzymatic domain.

1.9 Carbohydrate Binding Modules with chitin binding properties

CBMs with chitin-binding properties are found in CBM families 1, 2, 3, 5, 12, 14, 18, 19, 33 and 37. Chitin binding modules vary in size from 40-200 amino acids. Chitinase B used in this study has a CBM5 (Figures 1.6 and 1.8). The Chitin Binding Protein (CBP21) and the CBM33 from *E.feacalis* (EfCBM33), which are discussed in more detail below, are members of the CBM33 family. This family differs from the other CBM families as the majority of family 33 CBMs exists as individual entities. They are found in the genomes of most chitin degrading bacteria and are also identified in insect viruses (Vaaje-Kolstad 2005). Recently, the mechanism of CBM33 secreted by bacteria (discussed in chapter 1.12.2) has showed to use a mechanism that is both oxidative and hydrolytic (Forsberg et al. 2011; Vaaje-Kolstad et al. 2010; Vaaje-Kolstad et al. 2011). Interestingly, it has been shown that CBM33s act synergistically with chitinases (Vaaje-Kolstad et al., 2005) and that at least some members of this family are not binding modules but enzymes (Vaaje-Kolstad et al., 2010).

1.10 Chitin Binding Protein 21

Chitin Binding Protein 21 (CBP21) is a member of the CBM33 family derived from *Serratia marcescens*. This enzyme acts on the surface of crystalline chitin where it breaks glycosidic bonds. This makes the substrate more accessible to hydrolysis by other enzymes such as normal chitinases, including Chi-B (Vaaje-Kolstad et al. 2005a; Vaaje-Kolstad et al. 2010). The CBP21 enzyme is quite different from chitinases, it does not show the characteristics for chitinase binding site; a groove or tunnel with surface exposed aromatic residues necessarily for binding (Vaaje-Kolstad et al. 2005b).

1.10.1 Structure

The CBP21 was the first protein in the CBM33 family that had a solved crystal structure. The crystal structure was solved by Vaaje-Kolstad et al. in 2005 at 1.55 Ångstrøm (Å) resolution (Vaaje-Kolstad et al. 2005b).

The CBP21 molecule consists of 197 amino acids and its structure is dominated by a fibronectin type III domain. This type of domain is evolutionary conserved and possesses two β-sheets forming a β-sandwich. In CBP 21 the sandwich consists of one three stranded β-sheet and one four stranded β-sheet.

CBP21 also has a bud, a so called pseudo-domain, consisting of three α-helices, one short α-helix and two 3_{10} α-helices, that are inserted between β-strands one and two in the FnIII fold. 3_{10} helices are rare compared to the normal α-helix. While the α-helix usually has a hydrogen-bonding pattern that links the C = O of residue *i* to the H – N group of residue *i* + 4 the 3_{10} helix has hydrogen bonding between *i* and *i* +3 (Lesk 2004).

CBP21 has a conserved metal binding site for divalent cations that comprises two histidines, His 114 and His 28 (Figure1.9) Available data so far indicate that the binding site is promiscuous, meaning that the need for divalent cations is unspecific. The activity of CBP21 is inhibited if metals are removed by EDTA and can be restored by adding a variety of divalent metals, including Zn^{2+} or Mg^{2+}.(Vaaje-Kolstad et al. 2010) ; for more on metal promiscuity see also Harris et al., 2010).

The substrate-binding surface of CBP21 (Figure 1.9) differs from other CBMs. While most CBMs have a binding surface dominated by exposed aromatic amino acids, the binding site of CBP21 consists of an area with highly conserved, hydrophilic residues pointing into solution. The importance of theses hydrophilic residues for activity was demonstrated by Vaaje-Kolstad et al. in 2005b. Six of the polar, hydrophilic side chains were mutated; while each of these mutants displayed only moderate reductions in chitin binding affinity, two of them showed a significant reduction in their ability binding capacity. It should be noted that the structural work on CBP21 showed that conserved aromatic residues previously thought to interact with the substrate are situated in the hydrophobic core of the protein (Figure 1.9)(Vaaje-Kolstad et al. 2005a; Vaaje-Kolstad et al. 2005b).

The binding site of CBP21 differs from other CBMs. While most CBMs have a binding site consisting of aromatic amino acids on the outside of the molecule, the binding site of CBP21 consists of an area with highly conserved, hydrophilic residues facing the solution. The importance of theses hydrophilic residues was demonstrated by Vaaje-Kolstad et al. in 2005. Six of the polar, hydrophilic side chains were mutated and all mutants showed reduced binding affinity towards chitin. The same study also showed that eight conserved aromatic residues previously thought to interact with the substrate were situated in the hydrophobic core of the protein; Trp-94, Trp-108, Trp-119, Tyr-121, Trp-128, Trp-178, Phe-187, and Tyr-188 which are colored pink in figure 1.14 (Vaaje-Kolstad et al. 2005a; Vaaje-Kolstad et al. 2005b).

CBP21 contains two disulfide bridges one, between Cys-41 and Cys-49, in the loop/helical region and one joining β-strands 4 and 5 in the FnIII domain Cys-145 and Cys-162 (figure 1.9) (Vaaje-Kolstad et al. 2005b).

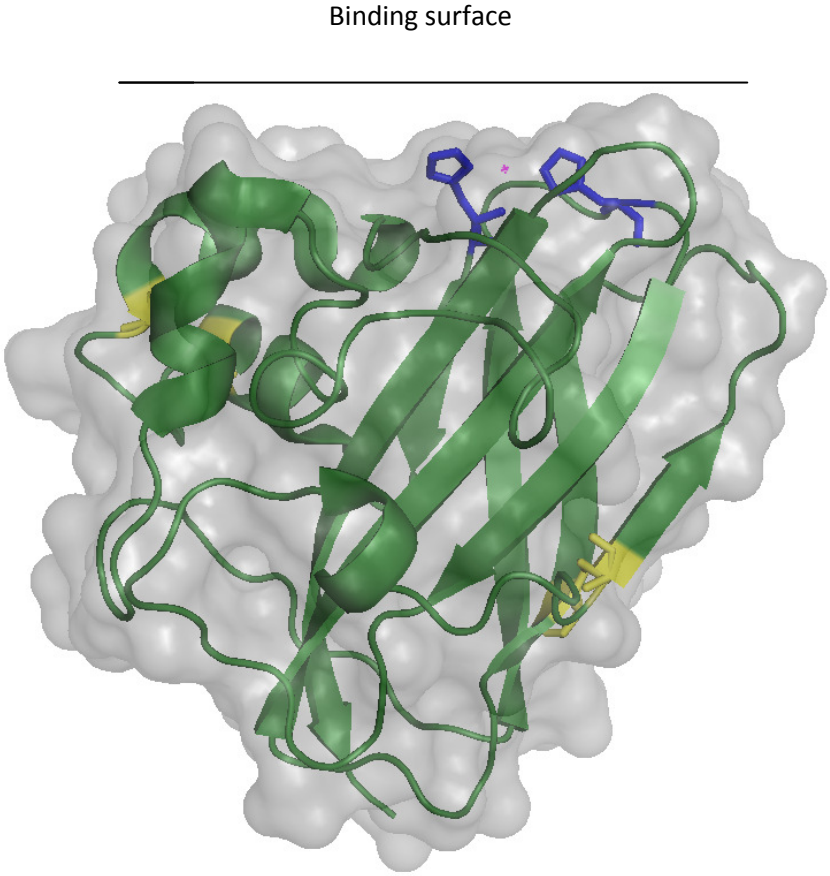

Figure 1.9: Structure of CBP21 (PDB code 2BEM) an oxidative enzyme in the CBM33 family. The side chains of the two conserved histidines forming the metal binding site are shown as blue sticks with a sodium-ion (magenta) between them. Disulfide bridges are shown as yellow sticks. Picture made with PyMOL (DeLano 2002)

1.10.2 Catalytic mechanism

Degradation of chitin by CBP 21 includes hydrolysis of glycosidic bonds which is accompanied by oxidation of the crystalline surface of chitin (Fig. 1.10). The newly generated chain end that would be called “reducing end” if the CBP21 were to be a normal hydrolytic enzyme becomes oxidized. Because of this Vaaje-Kolstad et al suggested to call CBP21 a”chitin oxidohydrolase” (Vaaje-Kolstad et al. 2010). The action of CBP21 destroys or disrupts the crystalline surface in a way that is not completely understood so that the crystalline chitin becomes more accessible to the chitinases, which degrade the chitin further. It is assumed that CBP21 binds chitin, cuts it and releases the substrate completely before it moves to a new location on the crystal (Vaaje-Kolstad et al. 2010).

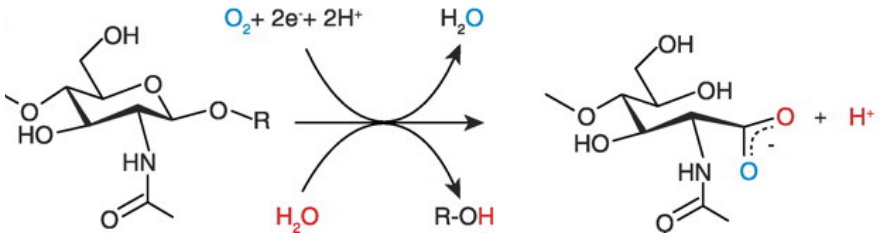

Figure 1.10: Schematic illustration of the enzymatic reaction catalyzed by CBP21. In the final oxidized product, one oxygen comes from molecular oxygen (blue) and one from water (red) (Vaaje-Kolstad et al. 2010).

1.11 Carbohydrate Binding Module 33 from *Enterococcus faecalis* (EfCBM33)

The CBM33 enzyme encoded by gene *ef_0362* referred to in this thesis as EfCBM33, is secreted from *Enterococcus faecalis* and exhibits the same mechanism as CBP21 that involves both hydrolysis and oxidation. The mechanism of EfCBM33 was recently solved by Vaaje-Kolstad et al. in 2011. In this (unpublished) work its crystal structure was solved, showing a similar structure resemblance to CBP21 (Vaaje-Kolstad et al. 2011) (figure 1.11). In this thesis EfCBM33 has been used as a comparison study, to look at the thermo-stability between EfCBM33 and CBP21.

EfCBM33 is active on both α- and β- chitin in a hydrolytic and oxidative manner and just like CBP21, EfCBM33 boosts the enzymatic chitinase (EF0361) secreted by *E.faecalis.* EfCBM33 are missing the two disulphide bridges found in CBP21, which is often conserved in the CBM33 family (Bøhle et al. 2011).

1.11.1 Structure of EfCBM33

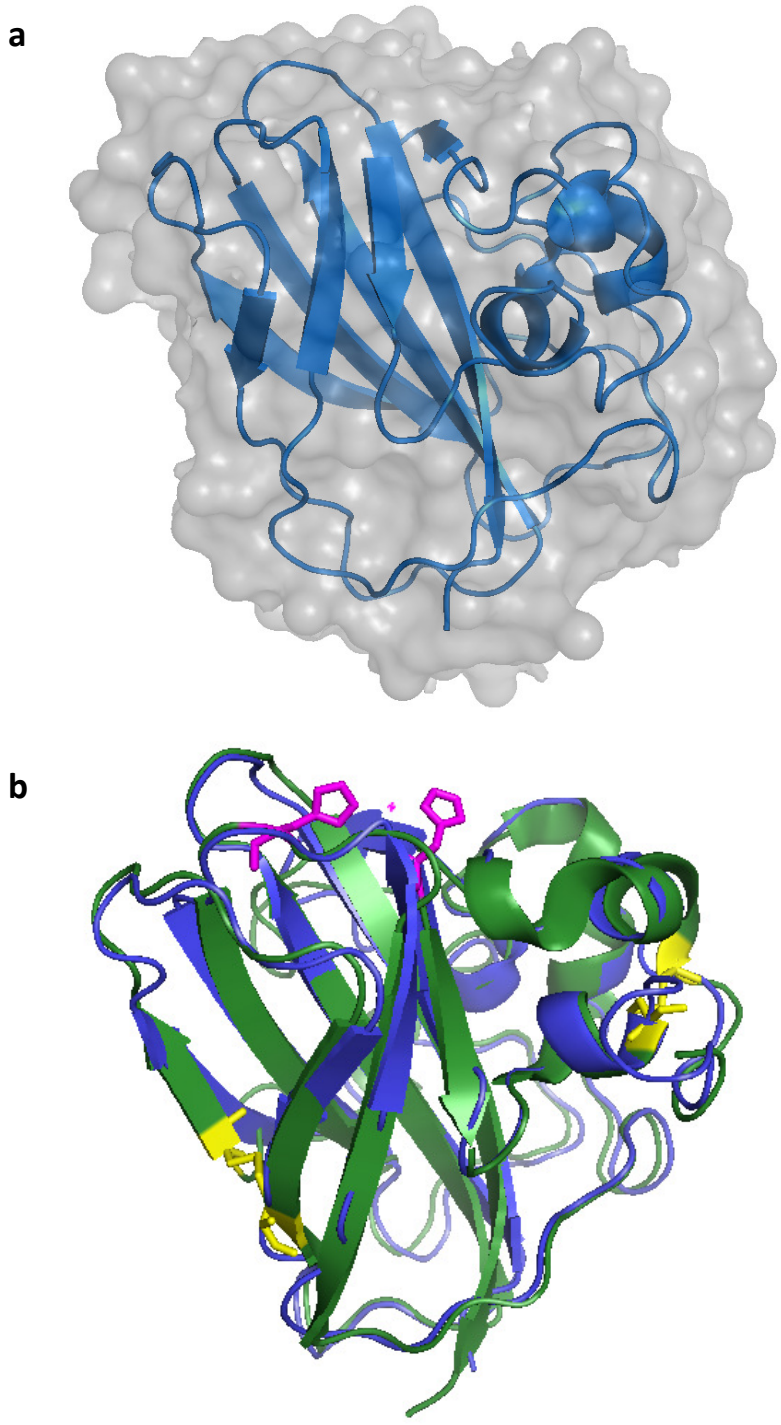

Figure 1.11: **The structure of EfCBM33** (a) Ribbon representation of EfCBM33 surrounded by a semi-transparent van der Waals surface. (b) Structural alignment of CBP21 (green) and EfCBM33 (blue). The histidines in the metal binding site of CBP21 (His 114 and 28) are shown as sticks (magenta), while the disulphide bridges (Cys-145 and-162 + Cys-41 and -49) are shown in yellow (also in CBP21). Picture made with PyMOL.

1.12 The chemical structure of proteins

In order to evolve more stable proteins one needs to understand how proteins are built up and the internal forces that determine the protein fold and its resistance against unfolding.

Natural proteins are normally built up of twenty natural amino acids. All amino acids found in proteins encoded by the genome have an L-configuration.

The amino acids are joined together by peptide bonds to form a polypeptide, the primary structure of a protein. The side chain (R) is attached to the C_α. Ignoring the R groups, the polypeptide creates the backbone of the protein, a linear main chain consisting of $(–N\text{-}C_\alpha\text{-}CO\text{-})_n$.

The side chain of an amino acid is what makes the amino acids differ from each other. The side chains, which are also called resides (R), can be divided into different categories such as polar, hydrophobic or charged residues.

The structural arrangement of all protein atoms in three-dimensional space is referred to as the protein structure or configuration. This configuration is influenced by many factors, including steric effects of the atoms, which means that every atom in a molecule occupies a certain amount of space. Other factors include the many types of interactions that occur in proteins, including hydrogen bond formation, charge-charge interactions and van der Waals interactions (Lesk 2004).

There are three different types of bonds in the main chain of a polypeptide, the N-C_α bond, the C_α-C bond and the peptide bond (C-N). The rotation angle (or “torsion angle”) for the N-C_α bond is named phi (ϕ), while the rotation angle for the C_α-C bond is named psi (ψ). The conformation of the protein is primarily determined by rotation around these bonds, which are single bonds. ϕ and ψ’s internal rotations are restricted by possible steric hindrance caused by the side groups of the two bonded atoms. In a Sasisekharan-Ramakrishnan-Ramachandran plot, ϕ and ψ angles can be plotted each point in the plot representing a C_α and the ϕ and ψ angles on either side of that atom. Here one can see ϕ,ψ combinations cluster up in popular regions, also called allowed regions. Ramachandran plots can be used for quality control of structural models, since the presence of many “non-allowed” ϕ,ψ combinations may indicate errors. They can also be use in the design of mutations, to check whether

mutations seem feasible in terms of the ϕ,ψ combination at the mutated site. The latter is of particular importance when the mutation involves residues with exceptionally wide (Gly) or exceptionally narrow (Pro) allowed ϕ,ψ combinations.

The rotation angle of the peptide bond is named omega (ω). The peptide bond is partially double bonded and basically has only two possible conformations, *trans* and *cis* (i.e. no real free rotation). The trans conformation around the peptide bond has a angle of rotation at 180°. The *cis* conformation has an angle of rotation at 0° and is an unfavorable conformation except in front of a proline appears. Most *cis* conformations appear before a Proline because the energy difference between *cis* and *trans* is less for proline residues than for the other amino acids (Lesk 2004)

The peptide bond is a rigid planar entity and how much twist there is in ϕ and ψ defines how one amide plane is going to sit relative to the adjacent amide plane. This twist of ϕ and ψ is called torsion angels.

Side chains in a protein in principle have the ability to adopt a large variety of conformations, but, due to steric restrictions, most side chains have clear repertoires of preferred conformations. Such preferred conformations are referred to as rotamers and these can be assembled in rotamer libraries. Such libraries are important in mutant design since it is important to check that the space that is available in the protein to be introduced side chain is compatible with this side chain adopting a favorable rotamer (Lesk 2004).

1.13 Protein stability

Protein structures are stabilized by several factors including covalent chemical bonds, hydrogen bonding, Van der Waals forces and the hydrophobic effect. Their stability is determined by the overall difference in free energy between folded and unfolded forms (Matthews et al. 1987). Lack of sufficient stability in enzymes limits their industrial use because of reduced lifetimes. Furthermore, running a process at higher temperatures usually reduces process costs

This section describes some of the factors that affect protein stability, with special focus on factors relevant for the enzymes (EfCBM33 and CBP21) whose stability has been analyzed in this study.

1.13.1 Entropic stabilization

Entropy (S) was first defined in the context of heat, explaining how two systems in contact with each other spontaneously would transfer heat to the colder system. Today the entropy term covers more (Atkins & De Paula 2006; Lesk 2004). When looking at entropy in the context of proteins, one can also see it as a measure of the amount of conformational freedom a system has. A system will always seek the state where it has the greatest possible conformational freedom (Atkins & De Paula 2006). In a protein context this means that entropy drives the protein towards unfolding, since the unfolded state has much more conformational freedom than the folded state.

Entropic stabilization is one of the most promising strategies for the stabilization of proteins by decreasing the entropy of the unfolded state of the protein. It is easy to evaluate and do not induce unfavorable strain in the folded protein structure. The challenge of entropic stabilization is to avoid negative effects of steric overlapping and to assure that the stabilizing effects does not lead to the inactivation of enzyme (Eijsink et al. 2004).

Every residue in a protein contributes more or less equally to the configurational entropy of folding/unfolding of a poly peptide back bone, except glycines and prolines. Glycine (Gly) is the most flexible amino acid when it comes to configurational energy, due to its lack of a β-carbon. Because of this, Gly will require more free energy to be folded into a native protein than Alanine (Ala) (Matthews et al. 1987). Proline is conformationally restricted compared to the other amino acids due to its pyrolidine ring. Therefore, Pro requires less free energy to be folded into a native protein than Alanine (Ala). Therefore, as originally shown by Matthews et al. (1987) proteins may in principal be

stabilized by replacing glycines and by inserting prolines. Both types of mutations reduce the entropy gain of unfolding.

A special variant of entropic stabilization concerns disulfide bridges. A disulfide bridge is formed between cysteine residues and is one of the simplest examples of post translational modification. In unbound form cysteine is a highly reactive amino acid vulnerable to oxidation, but in folded proteins, these residues usually form disulfide bridges. Disulfide bridges are formed between two cysteins by oxidation to form covalent bonds. The presence of these bridges reduces the entropy of the unfolded state relative to the folded state and thus, these bridges may stabilize proteins (Eijsink et al., 2004). Although free cysteines are unstable, it has been shown that disulfide bridges may withstand harsh conditions and can contribute to protein stability even at very high temperatures (Mansfeld et al., 1997; Eijsink et al., 1998).

Entropic stabilization is one of the most promising strategies for the stabilization of proteins and literature contains many examples of successful use of this strategy for generating stable protein variants (Eijsink et al., 2004). Possible structural effects of Gly->Ala and Ala-> Pro mutations are relatively easy to evaluate adding confidence to mutation design. The challenge of these two types of entropic stabilization is to avoid negative effects of steric overlapping and stress caused by torsion angle limitations (Eijsink et al. 2004). Design of stabilizing disulfide bridges is less straightforward, but several successful examples have been described (e.g. Mansfeld et al., 1997; Bjørk et al., 2003).

1.14 Mutant design by comparing naturally occurring variants with varying stabilities

To obtain a more thermo-stable enzymes one can look for homologues in organisms that grow under extreme thermal conditions. Most bacteria can grow over a wide temperature range, but they usually have a narrower range for optimal growth. The majority of bacteria are mesophilic, meaning that they grow optimally in the temperature 30 - 37 ^{o}C range. Psychrophiles are species that have temperature optima around 15-20 ^{o}C but can also grow at temperatures around 0 ^{o}C. Bacteria are called thermophilic if their optimum growth temperatures are in the 50-55 Celsius range (Degré 2000). Hyperthermophiles, sometimes called extreme thermophiles, grow at even higher temperatures sometimes even above 100 ^{o}C. Most of the hyperthermophilic microorganisms live in hot springs containing sulfur, which is essential for their metabolism (Tortora et al. 2007). Thermophilic bacteria produce various proteins that can withstand higher temperatures than their homologues produced by mesophilic bacteria. Sequence and structural comparisons of naturally occurring (more and less) stable variants of the same protein can yield suggestions for mutations that will stabilize the mesophilic variant. It should be noted, however, that it is not straightforward to recognize such stabilizing mutations, not even when structures of the proteins in question are available (Eijsink et al., 1995, 2004).

1.15 The consensus approach

The consensus approach is based on the theory that conserved residues in homologous proteins contribute more to stability compared to residues that are not conserved. It is thought this might be due to the fact that all homologues are derived from a common thermophilic ancestor. Therefore, by combining conserved residues in one mutant, highly stable protein may sometimes be obtained (van den Burg & Eijsink 2002), as has been shown for fungal phytases (Lehmann et al. 2000),3-isopropylmalate dehydrogenase (Miyazaki et al. 2001) and staphylococcal nuclease (Chen & Stites 2001).

1.15.1 Metal binding

Some proteins bind metal ions that may contribute to stability and/or have a catalytic role (Dionisi et al. 1999; Harris et al. 2010; Kozlowski et al. 2008; Page & Di Cera 2006; Vaaje-Kolstad et al. 2010). Binding of metal ions may make protein structures more rigid, compact and stabile (Kristjansson & Kinsella 1991; Wei 1999).

Even though metal binding may be beneficial for stability and activity, it should be noted that metal ions may have negative effects at high concentrations because of a specific binding. In particular, too high concentrations may affect the proteins activity. How high metal concentrations a protein can tolerate is protein dependent and may vary.

Ca^{2+} is a well known stabilizer at high and low temperatures as for example shown by Chan et al. in 1996 who demonstrated that binding of Ca^{2+} stabilized a DNAse. This study also showed that not all metal binding sites are as promiscuous as the metal binding sites in CBM33 proteins: while Ca^{2+} stabilized the DNase, Mg^{2+}, Mn^{2+} and Zn^{2+} destabilized it (Chan et al. 1996).

1.16 Spectroscopic methods for characterizing proteins in solution

Increasing temperature is a common technique used to induce protein unfolding and thermal denaturation, and resistance towards temperature-induced unfolding is one of the most common parameters used to study protein stability. In this study two different spectroscopic techniques were used to monitor protein unfolding, fluorescence and Circular dichroism.

1.16.1 Fluorescence

Fluorescence is a technique useful for investigating the tertiary structure of proteins and to monitor how this structure is lost during heating. Fluorescence spectroscopy is a sensitive method meaning that low protein concentrations may be used.

Fluorescence means the loss of excitation energy, by the re-emission of absorbed light. The emitted light has lower energy (higher wavelength) due to partial loss of excitation energy to heat. The difference in excitation and emission wavelengths makes it possible to filter out the excitation light for the detection of fluorescence signal. The fluorescence signal is measured by the fluorescent intensity meaning the ratio between photons emitted and photons absorbed, a measure called the quantum yield (Lesk 2004).

Fluorescence of proteins is due to the presence of the aromatic amino acids tryptophan (Trp, W), tyrosine (Tyr, Y), and phenylalanine (Phe, F). The aromatic amino acids all absorb light in the ultraviolet region of the spectrum, in the near-UV(Lesk 2004).

Table 1.4: The aromatic amino acids absorbs light at different wavelengths

Side chain	Absorption band (nm) = Excitation	Emission (nm)
Phenylalanine (Phe)	<257-279>	
Tyrosine (Tyr)	<274-294>	345
Tryptophan (Trp)	<280-300>	345

Tryptophan possesses the highest absorption coefficient, while Tyrosine comes in second and Phenylalanine has the lowest. When excitation wavelengths of 280 nm or higher are used, phenylalanine does not significantly contribute to the absorption and fluorescence signals.

Sometimes an excited molecule can transfer its energy to another molecule, which again may lead to the loss of emitted light, so-called quenching of the excited fluorophore (Jiskoot & Crommelin 2005).

Many proteins, including CBP21 and EfCBM33, contain both tyrosine and tryptophan, and the simultaneous emission of these two fluorophores may lead to complicated fluorescence data, due to resonance energy transfer from Tyr to Trp and deprotonation of Tyr. Tryptophan can selectively be excited at wavelengths between 295 and 300 nm and, therefore, use of these wavelengths yield simpler and “cleaner” signals. In contrast to tyrosine and phenylalanine, tryptophan emission is highly dependent on the polarity of the environment of the fluorophore (Jiskoot & Crommelin 2005; Righetti & Verzola 2001). Therefore, monitoring of tryptophane fluorescence provides an excellent method for measuring protein unfolding. For example, unfolding of CBP21 will lead to tryptophans (Fig. 1.12) moving from the hydrophobic interior of the protein to a solvent-exposed state.

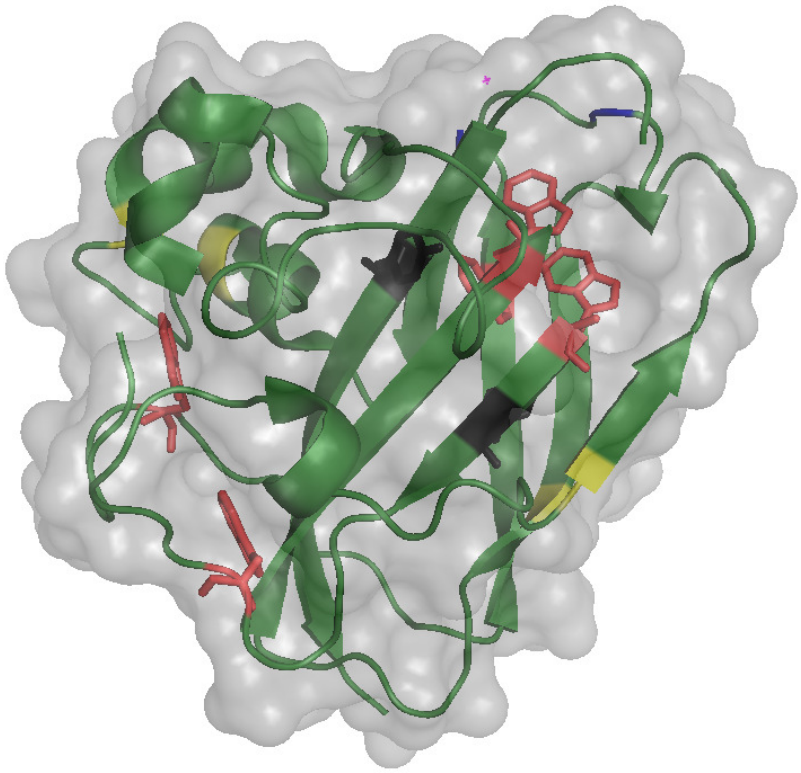

Figure 1.12: The structure of CBP21 (PDB entry 2BEM). The conserved aromatic residues are shown as sticks, tyrosine (black) and tryptophan (red). The histidine-residue motif, sodium-metal and disulfide bridges are shown in the same color as figure 1.9. For illustration purposes the residues isoleucine-180, serine-118 and glutamine-88 from the main chain were removed. Picture made with PyMOL (DeLano 2002)

1.16.2 Circular dichroism

Circular dichroism (CD) is a technique for examining protein secondary structure or tertiary structure in protein. Since proteins are chiral objects, their secondary structure content can be measured quantitatively by using circular dichroism. In this thesis CD was used to validate the findings from the fluorescence emission experiments.

In CD, plane polarized light passes through the chiral medium, which affects the plane of orientation to reorient a process called optical rotation. In addition there is some loss of orientation, called elipticity, which is observed in circular dichroism.

CD spectra may be divided into three regions: The far UV region (180-250nm), the near UV region (250-300nm), and the UV – vis region (300-700nm). The far UV signal yields information about the secondary structure of the protein and can in principle be used to determine the secondary structure composition of a protein. In this study the CD-signal at 222nm, often considered as a measure of helicity, was used to monitor unfolding. This is not optimal for proteins such as CBP21 that consist almost exclusively of beta-strands, but changes in beta-strands do in fact also affect the 222 nm signal.

1.17 Ultra High Performance Liquid Chromatography (UHPLC)

UHPLC is an instrumental analysis technique and method used for separation of chemical substances such as fatty acids, amino acids, proteins, hydrocarbons and nucleic acids. The substances to be separated are distributed between a stationary and a mobile phase and separated due to their physiological and chemical properties.

The instrument (a liquid chromatograph) consists roughly of a mobile phase, high pressure pump, injector, separation column with the stationary phase, detector and a computer system. The column is packed with very small particles to get good separation of the chemical substance and a high pressure is applied thru the system by the pump to separate the reaction mixture. UHPLC uses a higher pressure than conventional HPLC, which gives a better yield of separated components (Wren & Tchelitcheff 2006).

The separation of molecules occurs when the various substances in the sample will move at different speeds through the column because of different degrees of affinity to the stationary phase. The substances with greatest affinity will be retained in the column for a longer time than the ones with less affinity. Hydrophilic interaction (HILIC) separates polar compounds based on polar differences, and is a commonly method used to analyze monosaccharides, disaccharides, oligosaccharides and polysaccharides (Waters 1995).

The retention time (the time the molecule takes to eluate) can be time dependent. For example, a dimer of the crystalline chitin will come out after approximately one minute. The mobile phase can be held constant or it can be varied as a gradient. The separated components are detected by the detector, usually a UV detector as in the experimental work of this thesis.

1.18 Objectives of thesis

Chitin binding protein 21(CBP21) is an enzyme in the CBM33 family, that is capable of degrading β-chitin in an oxidative and hydrolytic manner. The CBM33 proteins act synergistically with classical hydrolytic enzymes and their use may speed up enzymatic degradation processes. One of the most important characteristics of enzymes for industrial processes is their stability. Therefore, the primary goal of this study was to study the thermo-stability of CBM33 proteins, with focus on the best known CBM33 member, CBP21. For comparison, stability studies of another CBM33, EfCBM33, were also conducted. Since stability alone is not enough for an enzyme to be successful, functional studies were also conducted. In particular, attempts were made to develop a new type of binding assay.

In order to analyze the functionality of CBP21 we have tried to develop a novel method formeasuring CBP21 binding to β-chitin based on the use of fluorescence. The goal was to develop a more efficient and sensitive assay by online monitoring of fluorescence signals as the enzyme binds to the β-chitin.

The goals of the thermal-stability study were to

- Characterize the two wild-type CBMs using both fluorescence and circular dichroism to monitor unfolding and to see if both spectroscopic methods worked equally well for monitoring stability.
- Study the effects of adding divalent metal ions on CBM33 stability.
- Study the effects of the reducing agent DTT that brakes the disulphide bonds present in CBP21 only

And, most importantly,

- To engineer more stabile variants by introducing designed single site directed mutations into CBP21.
- The thermo-stability studies provide insight into the stability of CBM33s at higher temperatures, whereas the designed mutations how single site mutations can provide increased stability to this important class of enzymes.

2. Materials

2.1 Laboratory equipment

Equipment	Brand
Chitin column: Econo-Column Flow Adaptor	Bio RAD
Chromatography instrument: Bio Logic LP	Bio RAD
Fraction collector: Bio Frac fraction collector	Bio RAD
Special lens-cleaning tissue	Assistent
Uv photometer: BioPhotometer, 8.5 mm	Eppendorf
Plastic disposable cuvettes: Plastibrand®	Brand
Precision cells made of quartz: SUPRASIL®, 10mm	Hellma
Cuvette: UVette® 220-1600 nm, RNase-/DNA-/protein- free	Eppendorf
Centrifuge 5430R	Eppendorf (big)
Centrifuge: Avanti™ J-25 centrifuge	Beckman coulter (Biggest)
Centrifuge 5415R	Eppendorf (little)
Incubator: watherbath SWB	Stuart
NuPAGE® 10 % Bis-tris Gel, 1.0 mm x 10 well	Invitrogen
Filter: filtroporus, 0.20µm, non pyrogenic sterile-R	Sarstedt
Centrifugal filter: Amicon® Ultra, Ultracell 10K, regenerated Cellulose 10,000 MWCO	Millipore
Sterile tube: Cellstar, greiner	Bio-one
pH meter: 827 pH lab	Metrohm Swiss made
Fluorometer: Cary Eclipse fluorescence spectrophotometer	Varian
Temperature controller: carry	Varian
Incubator: Multitron eco	Infors
Program: CaryEclipse Win FLR, thermal	Varian
Thermal cycler(PCR)	VWR
0.2 ml PCR tubes	Axygen®
1.5 ml sequencing tubes	Eppendorf
Syringe	BD Plastipak™
Syringe needle	BD microlane
Pipettes	finnpipette®
UHPLC	Agilent technologies

2.2 Chemicals

Chemicals	Brand
Agarose, SeaKem®	Lonza
Acetic acid (glacial) 100 %	MERCK
Acetonitrile CH_3CN	Fulltime chemical
Ammonium sulphate	MERCK
Ampicillin Sodium Salt	Sigma-ALDRICH
Bacto™ Tryptone, Pancreatic Digest of Casein, BD	Becton, Dickinson and company (BD), Difico laboratories
Bacto™ yeast extract, extract of autolysed yeast cells	Becton, Dickinson and company (BD), Difico laboratories
Bench mark™ Protein ladder	Invitrogen
β-chitin	France chitin
Bovine serum albumin (BSA) 100x	New England BioLabs
Calcium Chloride Anhydrous	SDS
Chitin beads stored in 20 % ethanol	BioLabs
Coomasie brilliant blue G250	BDH, Biochemical
Distilled water: Q guard, 0.22 µm, millipack 40	Millipore
di-Sodium hydrogen phosphate dihydrate $Na_2HPO_4*_2H_2O$	Merck
DNA polymerase Phusion	Thermo scientific
Ethylenediaminetetraacetic acid (EDTA) $C_{10}H_{16}N_2O_8$	VWR™ International AS
Gel loading Dye Blue (6x)	BioLabs New England
Glycerol 85 %	MERCK
Isopropanol	Vinmonopolet A/S
L-ascorbic acid	Sigma life sciences
L-Glutathione, reduced 98 %	ALDRICH
Magnesium Chloride-Hexa hydrate	MERCK
Methanol	MERC
3[N-Morpholino]propanesulphonic acid) sodium salt (MOPS)	Sigma
NuPAGE® Antioxidant	Invitrogen
NuPAGE® LDS Sample buffer (x4)	Invitrogen
NuPAGE® Sample reducing Agent (10x)	Invitrogen
Quick Change multi Site direced Mutagenesis kit	Agilent technologies
Sodium dihydrogen phosphate monohydrate, $NaH_2PO_4*H_2O$	Merck
Sodium Chloride	MERCK
Trizma ® Base, Primary standard and Buffer ≥99.9 % titration	Sigma life science
Zink di-Chloride $ZnCl_2$	VWR™ International AS
BigDye Terminator v3.1 Cycle Sequencing Kit	AB Applied Biosystems

3. Methods

3.1 Over expressing CBP21, Chi-B and EfCBM33 in *Escherichia coli*

3.1.1 Culturing of bacteria

The wild-type chitinase gene *chib* and the wild-type CBP21 gene *cbp21* gene from *Serratia marcescence* strain BJL200 were expressed in *Escherichia coli* TOP10 cells, while mutant variants of CBP21 were expressed in *Escherichia coli* XL1-blue cells. The gene encoding wild-type EfCBM33 was also expressed in *Escherichia coli* TOP10 cells. *E.coli* was cultivated in LB-media containing ampicillin. *E.coli* strains were stored in glycerol in a -80 °C freezer

Materials and reagents

LB-medium pH 7

10 g/l sodium chloride

10 g/l Bacto Tryptone

5 g/l yeast extract

Ampicillin

E.coli cells

Method

The *E.coli* cells were spread out on LB medium plates containing 50µg/ml ampicillin and 1.5 % agar and the plates were incubated over night at 37°C. A pre-culture was made by inoculation of one colony in 4 ml liquid LB medium containing 50 µg/ml ampicillin followed by incubation for 16 hours with shaking at 225 rpm, 37 °C. -80 stocks were prepared by adding 300µl sterile 87 % glycerol to 1.0 ml of the pre-culture. Additionally, for protein production, 1 ml of the pre-culture was transferred to 300 ml LB-medium in sterile 2 L culture flasks and the cultures incubated for another 16 hours with 225 rpm shaking in 37 °C. Work on bacterial cultures was performed in a sterile fume hood.

3.1.2 Periplasmic extract

The expression vectors for the two CBM33 proteins are constructed in such a way that the CBM33 proteins are exported to the periplasmic space, i.e. the space between the outer membrane and the plasma membrane in Gram-negative bacteria. To purify the proteins, the cells were exposed to high sugar concentration, followed by re-suspension in cold water. This treatment causes a cold osmotic shock which releases the proteins in the periplasmic-space without destroying the inner membrane (Brurberg et al. 1996; Manoil & Beckwith 1986).

Materials and reagents

Spheroplast buffer

34.2 g sucrose

20 ml Tris-HCl pH8

500 µl protease inhibitor

200 µl 0.5 M EDTA

dH_2O to 200 ml

20 mM $MgCl_2$

Method

After cultivation the bacterial suspension was stored on ice for 20 minutes in centrifuge tubes. Bacteria were then separated from the supernatant by 10 min centrifugation at 5000rpm, in a JA-10 rotor, at 4°C. The supernatant was thrown away, and the pellet re-suspended in 15 ml ice-cold spheroplast buffer and stored on ice for 5 minutes. The mixture was then spun down at 8000 rpm for 10 minutes at 4°C degrees. The supernatant was thrown away and the remaining pellet warmed up to room temperature, after which the pellet was re-suspended in 10 ml ice cold water and 1 ml 20 mM $MgCl_2$. After keeping the cells on ice for 45 seconds, they were spun down at 8000 rpm for 10 minutes at 4°C degrees. Now the proteins of interest were in the supernatant so this was kept as the periplasmic extract. The extract was filtrated through a 0.22 µm sterile filter and stores at 4 °C.

3.2 Purification of CBP21, EfCBM33 and Chi-B

3.3.1 Affinity chromatography with chitin beads

Affinity chromatography uses the specific biological or chemical interaction between two compounds. Here the affinity between enzyme and substrate is utilized as a separation technique. When purifying chitin-binding enzymes with affinity chromatography, the stationary bed in the column consists of chitin beads, the mobile phase is a buffer while the sample is the periplasmic extract. The chitinases will bind to the chitin beads thereby separating them from the periplasmic extract (Burtis et al. 2001).

Materials and reagents

Column with an adaptor, Bio Logic Chromatography instrument, fraction collector

Periplasmic extract

0.3 M NaOH

20 % Ethanol

Buffer A

1 $(NH_4)_2SO_4$ in 20mM Tris-HCl pH8 for purification of CBP21 and EfCBM33
20 mM Tris-HCl pH 8 for Chi-B

Buffer B

20 mM acetic acid pH 3.6

Method

Depending on the amount of protein in the periplasmic extract, the column contained between 5-20 ml of chitin beads. 25 ml periplasmic extract was adjusted to the same concentration and pH as buffer A before loading onto the column. The column was packed with buffer A at 2.5 ml/min flow (the operating flow rate). When the bed height was stabilized and the system properly equilibrated, the periplasmic extract was loaded on the column at rate 2.5 ml/min. After all the sample was loaded onto the column, the column was washed with buffer A. Proteins were monitored by measuring UV absorbance at 280 nm and the wash with buffer A was continued until the system was equilibrated to a straight baseline. Elution of proteins from the chitin beads was done with buffer B and the proteins were collected in clean glass tubes. After usage the column was washed with 3 column volumes of water followed by a wash with 3 column volumes of 0.3 M NaOH to remove all protein. After washing with NaOH, the column was washed with 6 column volumes of water and then stored at 4 °C in 20% EtOH for re-use.

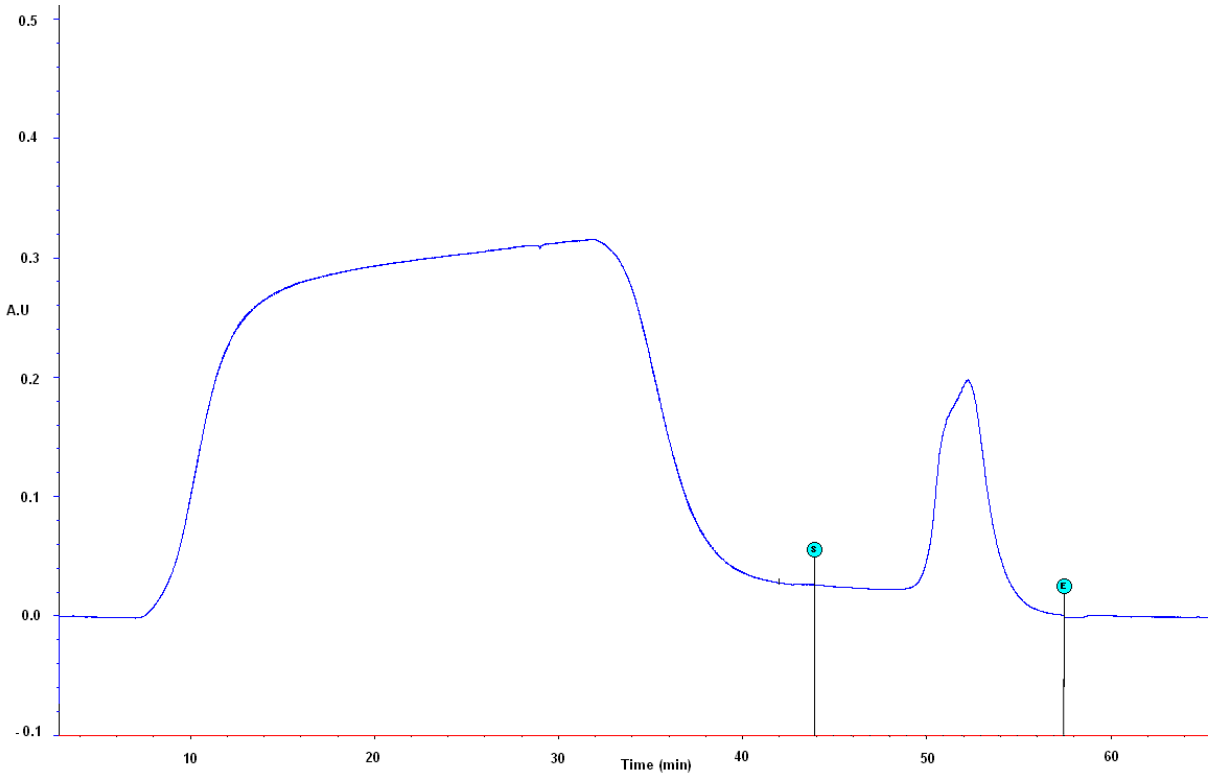

Figure 3.1: Typical chromatogram for purification of CBP21. The waste top (big top) elutes between 0 and 40 ml and CBP21 elutes at about 50 ml (small top). The start and stop point of eluent collection are shown on both sides of the eluent top (sticks with balls). The x axis showes the time of collection (min). Y axis shows the absorbance.

3.2.2 Sodium Dodecyl Sulfate-Polyakrylamid Gel Elektroforese (SDS-PAGE)

The purity of the purified proteins was analyzed using SDS PAGE, and gels were stained Coomasie blue for protein detection. The periplasmatic extract and a protein from an earlier purification were used as references for the interpretation of the gels.

To make sure that the proteins of interest actually exist and that there was no impurities, the purified protein were put on a SDS page gel and stained with Coomasie blue. The periplasmatic extract and a protein from an earlier purification were used as references for the interpretation of the gels. The SDS-staining procedure was also done on the periplasmic extract.

Materials and reagents

Protein solution for analysis

Protein Standard: Bench Mark Ladder

NuPAGE ® 10% Bis-Tris Gel 1.0 mm x 10 wellNuPAGE ® Sampelbuffer (4x)

NuPAGE ® Sample Reducing Agent (10X)

MOPS SDS Running Buffer

Sample buffer(stock solution)

5 µL NuPAGE ® Sampelbuffer (4x)

2 µL NuPAGE ® Sample Reducing Agent (10x)

3 µl distilled H_2O

Color Solution

Solution A:

50% 2-propanol 20% acetic acid

Solution B:

0.1% Coomassie Brillinat blue (in dH_2O)

De-staining solution

dH_2O- preferably hot

Method

10 µL protein solution was mixed with 5µl sample buffer (stock solution). The samples were heated at 90C° for 8 minutes to denatured proteins.

Pre-cast gels were placed in the tray in the electrophoresis camber. MOPS SDS Running Buffer was filled in the inner and outer electrophoresis camber and 5 µl protein standard and 20 µl protein samples were applied in their respective wells on top of the gel.

The gel was applied a voltage of 200 V and run for 50 minutes. After the separation of proteins, 25ml of solution A was mixed with 25ml solution B, heated in a microwave for 15-30 seconds and added to the gel. The staining solution was incubated for 1 hour and de-stained with hot dH_2O for 1 hour.

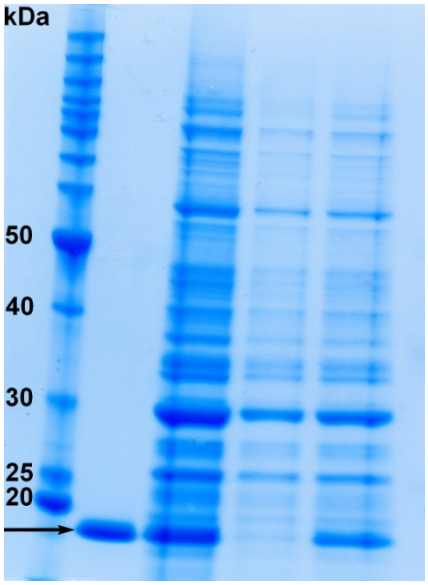

Figure 3.2: Purification of EfCBM33. Fraction 1=bench marck protein ladder, 2=purified protein, 3=periplasmic extract, 4+5=waste from the protein purification, to see how much EfCBM33 is lost into the waste.

3.2.3 Protein concentration determination

Protein concentration were done determined using Bio-Rad Protein assay, which is based on the method of Bradford. This assay utilizes the absorbance shift of an acidic dye from 465 nm to 595 nm upon binding to soluble protein. The linear range of the micro assay when using BSA as a standard is 1.2-10.0 µg/ml (Zor & Seliger 1996)

Materials and reagents

Coomassie® Brilliant Blue G-250 dye solution

Spectrophotometer set to 595 nm

Cuvettes with 1 cm path length

Bovine Serum Albumin from

Method

Standard curve

Five standards solutions of BSA were made in the range of 1.5-10 µg/ml. 800 µl of each standard and solution to be tested was dispensed into clean test tubes. The protein solutions were assayed in duplicates. Then 200 µl of the dye reagent concentrate were added to each tube, and the solutions were vortexed. The samples were incubated in room temperature for approx 5 minutes before measurements of the absorbance 595 nm. The BSA standards were first measured and concentration results were stored in the instrument as a standard curve, so that by the next measurement of protein concentration determination, only needed two parallels of a BSA standard as a control.

Measuring the samples

Depending on the amount of protein in sample, purified protein samples were diluted to appropriate concentrations in20 mM Tris pH 8. Two parallels were made for each protein sample. In addition to the protein samples two parallels of 10 µg/ml BSA standards were made. If the BSA standard deviated more than 5 % from the stored standard curve all the samples were discarded and the measurement repeated. If the measurements of the BSA samples still deviated from the standard curve, a new standard curve was made.

3.3 Mutant Design and construction

Attempts were made to increase the stability of CBP21 by introduction of site-directed mutations. Mutations were designed according to two principles. Entropic stabilization and the consensus approach (see section 1.13, 1.16). For the latter approach a multiple sequence alignment was constructed comprising five putatively thermo-stable proteins from the CBM33 family EfCBM33 and CBP21.

After identification of potential mutations (see section 1.15), the programs PyMOL and WHATIF were used to verify that mutations would not create problems in the structure. For mutations that seemed promising primers were designed and the template plasmid with *cbp21* gene was purified. After purification, site directed mutagenesis of the wild-type plasmid was carried out and the mutated plasmids were transformed into XL1-Blue cells grown on LB medium plates containing 50µg/ml ampicillin and 1.5 % agar. After growing cultures of individual transformants the mutated *cbp21* genes were sequenced.

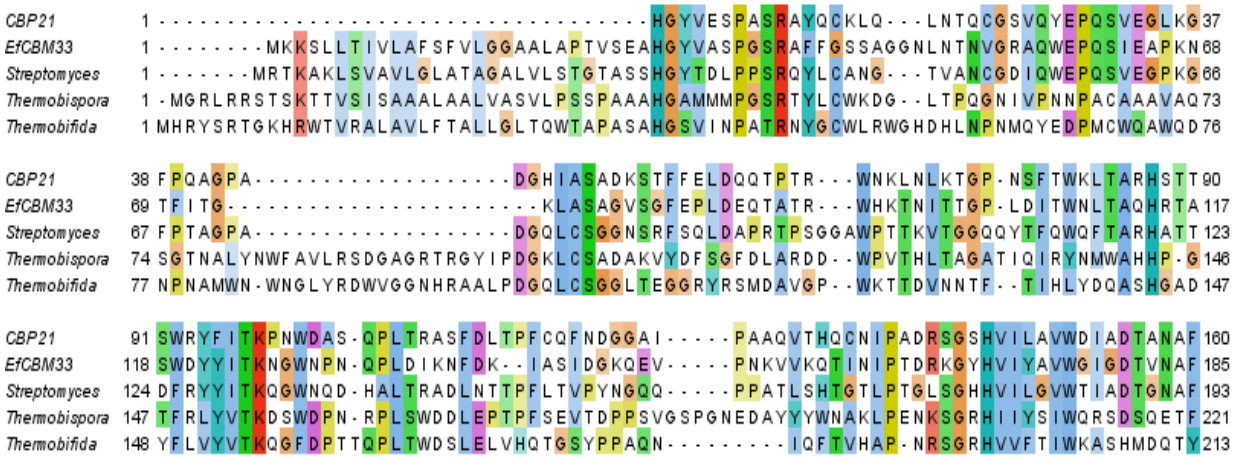

Figure 3.3: Sequence alignment of CBP21 and four CBM33 proteins. Mutations made in CBP21 from this alignment were G73A, A155P and A130P. The colors shown represent properties of the amino acid. The sequence alignment was made whit ClustalW2 (Larkin et al. 2007).

3.3.1 Harvesting plasmid from CBP21

Before proceeding with the site-directed mutagenesis, one needs to harvest the plasmid in which the mutation is carried out. The plasmid was purified by using the QIAprep® Spin Miniprep Kit, according to the manufacturer's instructions. The vector DNA contains an origin of replication that allows it to replicate independently of the host chromosome. The vector also has unique sites for the restriction enzymes so that the CBP21 gene can be inserted at a specific point in the vector that does not interfere with other functions.

Method

1–5 ml bacterial culture was incubated over night with shaking at 225 rpm and 37 °C. Then the bacterial overnight culture was centrifuged at >8000 rpm (6800 x *g*) for 3 min at room temperature.

The bacterial pellet was re-suspended in 250 µl cold Buffer P1 (stored at 4 °C and added RNase A), until there was no sign of cell clumps, and transferred to a micro centrifuge tube. 250 µl Buffer P2 was added and the reaction was mixed carefully by inverting the tube 4–6 times until the solution was clear. The lysis reaction was not incubated for more than 5 minutes.

350 µl Buffer N3 was added and mixed immediately and thoroughly by inverting the tube 4–6 times, until a cloudy suspension. The reaction mixture was centrifuged for 10 min at 13 000 rpm (~17 900 x *g*) in a table-top micro-centrifuge.

After centrifugation the supernatant was transferred to a QIA spin column and centrifuged for 1 minute at 13 000 rpm. The QIA spin column was then washed by 250 µl buffer PB (heated to 50 °C) to remove trace nuclease activity. The column was centrifuged for 1 minute in a micro-centrifuge.

An additional wash was performed by adding 0.75 ml buffer PE to the column with additional centrifugation at 1 minute. The flow thru was discarded and an additional centrifugation for 1 minute was performed. The QIA prep column was placed in a clean 1.5 ml eppendorf tube, and the DNA was eluted from the column by adding 50 µl buffer BE (10mM tris-HCl pH 8.5). The reaction was incubated for 1 minute and then centerifuged at 13 000 rpm.

3.3.2 Site directed mutagenesis

The mutations were made with the Quick change® multi Site-Directed Mutagenesis Kit, Revision C, from Agilent Technologies.

Materials and reagents

Thermal Cycler whit a hot-top assembly

0.2 ml PCR tubes from axygen®

14-ml BD Falcon polypropylene round bottom tubes

1 % agarose gel

LB-ampicillin agar plates

10 x Quick change® multi reaction buffer

dNTP mix

Quick change® multi Enzyme blend (polymerase)

Dpn 1 restriction enzyme

XL1-Blue super competent cells

pUC18 control plasmid (0.1 $\frac{\mathrm{ng}}{\mu\mathrm{l}}$ in TE buffer)

Plasmid: Double stranded DNA template (dsDNA) from CBP21 wild type provided from the Nucleospin procedure

Forward and reverse mutagenic Oligonucleotide Primers from eurofins

ddH_2O

1x TEA buffer

ethidium bromide

NZY^+ broth

Method

The sample reaction was prepared as indicated below in PCR 0.2 ml tubes. Mutant DNA was synthesized in a PCR reaction containing the template plasmid and two complementary primers containing the mutant sequence. Reaction mixtures were prepared as indicated below in 0.2 ml PCR tubes.

2.5 µl of 10 x reaction buffer

1.5 µl (52.5 ng) of dsDNA

1 µl (100 ng) of oligonucleotide primer forward

1 µl (100 ng) of oligonucleotide primer reverse

1µl of dNTP mix

ddH_2O to a final volume of 25 µl

After mixing these reagents 1µl of the Quick change multi enzyme blend (polymerase) was added

The sample reactions were incubated in a thermal cycler using these cycling parameters:

Segment	**Cycles**	**Temperature**	**Time**
1	1	95 °C	30 seconds
2	17	95	30 seconds
		55	1 minute
		68	1 minute/kb of plasmid length = 7 minutes

After amplification in the thermal cycler the reaction mixtures were placed on ice for 2 minutes and 1µl of each reaction mixture was then analyzed by agarose electrophoresis using 1 % agarose gels containing 2µl etidiumbromide solution.

Dpn I Digestion of the amplification products

1 µl Dpn I restriction enzyme (10 U/µl) was added to each of the amplification reactions, the solution was gently and thoroughly mixed by pipetting the solution up and down ten times. The reaction mixture was spun down in a micro centrifuge for 1 minute and immediately incubated at 37 °C for 1 hour to make sure the parental non mutated supercoiled dsDNA was digested.

Transformation of XL1-Blue supercompetent cells

The process of transformation involves introduction of recombinant DNA plasmid into the host cell. Treatment *E. coli* with Ca^{2+} makes the cells competent allowing the plasmid to pass through the cell membrane. This process is not yet fully understood but Ca^{2+} probably shields the negative charge on the DNA. The cells, now called transformants, are selected for by growing in ampicillin medium, which kills cells without the plasmid(Watson 2008).

The XL1-Blue super competent cells were gently thawed on ice to prevent lysis of the cells. For each control and sample to be transformed, 50 µl of the super competent cells were aliquot to pre-chilled 14-ml BD Falcon polypropylene round bottom tubes.

1 µl of the Dpn I treated DNA from each sample reaction was transferred to separate aliquots of the super competent cells. As a control to verify the transformation efficiency, 1 µl of the pUC18 control plasmid (0.1 ng/µl) was transferred to 50 µl aliquot of super competent cells. The transformation reactions were mixed by gently swirling and the reaction mixtures were incubated on ice for 30 minutes.

After incubation the transformation reactions were heat pulsed for 45 seconds at 42 °C and then placed on ice for 2 minutes. After 2 minutes on ice 0.5 ml of NZY^{+} broth preheated to 42 °C was added to each reaction and the transformation reactions were incubated at 37 °C for 1 hour with shaking at 225 rpm.

250 µl of each transformation reaction was then spread out on LB-ampicillin agar plates with 50 µg/ml ampicillin. For the pUC18 transformation control a 200 µl pool of NZY^{+} broth was placed on the

agar plate and 5 µl of the pUC18 control was placed whit a pipette into the pool and the mixture was spread out. The plates was incubated at 37 °C for >16 hours.

After incubation 3 colonies of the transformed cells was picked out with a toothpick and placed in separate tubes containing 4 ml LB- ampicillin broth ($50.0\frac{\mu g}{ml}$) and the transformed cells were incubated an additional 16 hours over night. After incubation 1 ml of the media was prepared as frysestokk and a second preparation of plasmid from the Nucleospin kit was used to purify the mutated plasmids. After purification 12 µl of the plasmids were placed on a 1 % agarose gel whit 2 µl ethidium bromide.

3.3.3 DNA sequencing

The reagents were provided from the BigDye® Terminator v3.1 Cycle sequencing kit.

There are three general steps in DNA sequencing; annealing, extension and denaturation. All three steps occur in a thermal cycler by adding DNA template, nucleotides (dNTPs), dideoxynucleotides (ddNTPs), primers, polymerase and buffer combined. The first step involves denaturation of DNA by heating. After denaturation and lowering of the temperature, the primer anneals to the DNA, DNA synthesis leads to sequentially adding of nucleotides to the 3'-hydroxyl end of the primer bound to the DNA template. The newly synthesized ssDNA strand is called the "extension product". The extension product grows in the 5'-3' direction by forming a phosphodiester bridge between the 3'hydroxyl at the growing end of the primer and the 5' phosphate group at the incoming dNTPs. The extension product is terminated by incorporation of a ddNTP. DNA synthesis is carried out amplified in the thermal sampler.

The sample reaction was prepared according to the protocol from Big Dye as indicated below.

Materials and reagents

Thermal cycler whit a hot-top assembly

0.2 ml PCR tubes from

Pipettes

2 µl mutated and purified plasmids

2µl Big Dye premix RR100/ Bigdye Terminator reaction mix

5 µl 5 x sequencing buffer

3.2 pmol pRSETB forward primer

3.2 pmol pRSETB reverse primer

ddH_2O to a final volume of 20 µl

Two tubes were needed for each mutated plasmid; one for the reverse primer and one for the forward primer.

Ethanol/EDTA precipitation

The Ethanol/EDTA (EtOH/EDTA) precipitation is a purification process to remove all excess color-labeled ddNTPs. In the EtOH/EDTA precipitation assay it is important to have high ethanol concentration, or else the extension product will not precipitate properly and extension product will be lost in the supernatant. This can also happen if the supernatant is not removed immediately after the 30 minute centrifugation.

Materials and reagents

125 mM EDTA

96 % ethanol

70 % ethanol

1.5 ml sequencing tubes

Method

The sample reaction was prepared as indicated below in 1.5 ml sequencing tubes.

The extension product was transferred to sequencing tubes, and then added 2µl 125 mM EDTA and 62.5 µl 96 % Ethanol. The reaction was mixed by inverting the tubes several times and incubated at room temperature for 15 minutes. The reaction mixture was spun down in a micro centrifuge at 4 °C for 30 min at maximum speed. The supernatant was immediately aspirated with a syringe needle attached to a water vacuum suction. 60 µl of 70 % ethanol was then added and the tubes were centrifuged again (maximum speed 10 minutes) followed by aspiration of the supernatant with a vacuum suction. To remove all excess liquid the tubes were dried in a vacuum centrifuge for 5 minutes.

Capillary electrophoresis

After EtOH/EDTA precipitation the products from the cycle sequencing reaction are injected into a capillary electrophoresis system. The products are injected into the capillary system because of electro kinetic injection; negatively charged fragments are forced into the system because of the pushing force of a high voltage. The labeled DNA fragments are indirectly separated by molecular weight; the total charge of the extension products separates them. Because of this the DNA fragments are indirectly separated by size. DNA fragments are then detected by a laser beam which causes the fragments to emit the fluorescent dye.

3.4 Thermo stability measurements

In this study, protein stability was measured by monitoring the effect of temperature on intrinsic fluorescence (theory described in section1.17.1) and circular dichroism (theory described in section 1.17.2). In standard experiments, the proteins were tested at different concentrations and heated from 20 °C to 80°C or 90°C and back to 20°C again, using a heating/cooling rate of 5 °C/min or 1°C/min. Subsequently, the samples were checked for the presence of precipitated material by sampling protein material and the possible occurrence of re-naturation after cooling down to 20°C and at further cooling to 0°C, and after prolonged storage for 24h at 4 °C. Refolding was checked visually by looking for aggregates in the cuvette.

Many of the chitin binding proteins unfold when exposed to high temperatures. In these proteins Tyrosine and Tryptophan exists mostly internally and can therefore be used as a signal molecule, in this case a fluorophore. When the proteins denature these amino acids are no longer hidden on the insides of the protein and can be detected in a flourospectrophotometer.

The proteins were adjusted to different concentrations and exposed to temperatures from 20- 90°C and back to 20°C again, 5 °C/min. After degradation the samples were checked for precipitation at room temperature and if there was any sign for renaturation of the protein after cooling down to 4°C.

3.4.1 Using intrinsic fluorescence to assay thermo-stability

The protocol for measuring unfolding of CBM33s by monitoring fluorescence was developed in this study. Therefore, initially, a wide variety of conditions were tested, varying parameters such as heating rates, protein concentrations, excitation wavelengths and maximum temperatures. This was done to determine the optimal conditions for obtaining interpretable unfolding curves. When the assay conditions were established unfolding assays were performed in 20mM Tris buffer pH8, and reactants such as divalent metals, DTT and EDTA were added to see if this would affect the apparent melting temperature (T_m^{app}) of the protein.

Materials and reagents

10mm precision cells made of quartz

20 mM Tris-HCl buffer pH8

Protein solution to be tested

$MgCl_2$, $CaCl_2$, $ZnCl_2$, DTT, EDTA

3M acetic acid

70% ethanol

Instrumentation and sofware

Fluorescence spectrophotometer with a temperature controller and a Xenon lamp from Cary Eclipse

The software used to measure the signals: CaryEclipse Win

Method development

The methods were developed using CBP21. The first experiments were done using a temperature range from 20 °C to 90 °C, a heating rate of 5 °C/min and a protein concentration of 1, 2 or 5 µM. The experiments with 2 µM protein gave the best results and this concentration was therefore used in al further experiments.

Excitation wavelengths between 280 nm and 295 nm were tried out. The wavelength of 295 nm showed the best unfolding curves, probably since this excitation excludes the excitation of tyrosine which may cause undesired complications of the fluorescence data (see section 1.17). The excitation wavelength of 295 nm was used in further unfolding assays.

Two heating rates were tried out, 1 °C/min and 5 °C/min. Use of the lower heating rate led to lower apparent Tm values, which was considered favorable. To give CBMs sufficient time to (hopefully) equilibrate, unfolding assay was carried out at 1 °C/min instead of 5 °C/min. Also, the 1 °C/min heating rate gave better results in turns of reproducibility.

Finally, the standard conditions for the unfolding assay of CBP21 by fluorescence were set to 2µM protein concentration, excitation wavelength at 295 nm and emission of 345 nm, heating rate of 1 °C/min and readings at 700 Volt while the temperature intervals were set to be 20-90°C or 20-80°C. These parameters were also used for EfCBM33.

Method

The reaction volume was set to 1 ml. Unfolding experiments was performed in by using two parallels of a reaction mixture that contained 2µM of protein in 20mM Tris-HCl pH8. The reaction mixture was incubated for approximate 10 minutes on the bench in order to obtain room temperature, before it was placed in the fluorescence spectrophotometer for the heating analysis.

To remove aggregates and protein leftovers, the cuvettes were carefully cleaned after each run. This was done by rinsing them in warm tap water (5 times), washing with a cotton swab, rinsing in warm water (5 times), soaking overnight in 3M acetic acid, rinsing well in tap water (10 times), rinsing in 70% ethanol (3 times), and, finally, rinsing in MQ water (10 times).

Reaction volume was set to 1 ml. Unfolding experiments was performed by using two parallels of reaction mixture that contained 2µM CBP21 wild-type, CBP21 mutants or EfCBM33 in 20mM tris-HCl pH8. The reaction mixture was incubated for approximate 10 minutes on the bench in order to obtain room temperature. At time points (1 °C/min) reaction mixture was read at excitation wavelength 295nm and emission of 345nm when heated from 20-90°C or 80°C in a fluorometer (Cary Eclipse).

To remove aggregates and protein leftovers, the cuvettes were carefully cleaned after each thermo-stability run. This was done by rinsing them in warm tap water 5x, wash with a cotton swab, rinse in warm water 5x, soak overnight in 3M acetic acid, rinse well in tap water 10x, rinse in 70% ethanol 3x, rinse in MQ water 10x.

Test of aggregation and refolding test

For testing aggregation and possible refolding, protein solutions were heated from 20 °C to 80°C at 1°C/min or 5 °C/min, after which the solutions were cooled down at the same rate as the heating rate to 20 °C, and further down to 0°C. 20 µl protein solutions were taken out from the cuvette at 80 °C, at 20°C and at 0°C. The 20 µl were spun down in eppendorf tubes in a micro centrifuge at 14200 rpm for 5 min. 10µl of the supernatant was transferred to an eppendorf tube after centrifugation. 10 µl SDS sample buffer was added to all tubes. The samples were run on a NuPAGE® Novex® 10% Bis-Tris Gels (Invitrogen, Life Technologies, Carlsbad, CA) following the standard procedure from the manufacturer, as described in section 3.2.2.

3.4.2 Calculation of apparent melting temperature (apparent T_m)

The apparent melting temperature (apparent Tm) calculated from the thermal stability assay gave an impression of when temperature of protein melting occurred. Apparent T_m was calculated to give a sigmoid curve, thereby making it easier to assume the melting point of the protein. In the case of CBP21 and EfCBM33 the melting temperature was dependent on the heating rate:

$$apparent\ T_m\ = \frac{Y_n - Y_{obs}}{Y_n - Y_d}$$

Where Y_n= value of y for the native part of the curve, Y_{obs}= observed fluorescence signal, Y_d= value of y for the denatured part of the curve (Pace 1990)

3.4.3 Using Circular dichroism to assay thermo-stability

Circular dichroism was measured to monitor unfolding of CBP21 wild-type and EfCBM33. See section 1.17.2 for further details

Materials and reagents

High precision Quartz cuvettes 20 mm path length

50 mM sodium phosphate buffer, pH 7.0

Purified CBP21 and EfCBM33

Method

The reaction volume was set to 200 µl. Unfolding experiments were performed by using protein concentrations of 2 µg/ml or 1 µg/ml in 50 mM sodium phosphate buffer, pH 7.0 in high precision quartz cuvettes. The reaction mixtures were measured at 222nm while being heated from 25 °C to 80 °C. When measuring the secondary structure content of the proteins, the samples were scanned from 190 nm to 260nm before and after heating. Signals (minima) at 208 nm and 222 nm indicate α-helical structure, whereas a minimum at 217 nm is characteristic of β-sheet (Woody 1995).

3.5 Binding assay to β-chitin

3.5.1 Binding assay

Binding assays were carried out as described by (Vaaje-Kolstad et al. 2005b). They were performed using β-chitin from squid pen as substrate and purified CBP21 wild type as enzyme. Binding of CBP21 was measured indirect by measuring reduction of the protein concentration in the supernatant at different time points, after incubation with β-chitin at room temperature.

Sample materials and reagents

UV BioPhotometer, from Eppendorf, Hamburg

Plastic disposable cuvettes: Plastibrand®

10 mg/ml stock suspensions of β-chitin (in double distilled H_2O), from squid bone from France Chitin

Double distilled H2O

50 mM sodium phosphate buffer, pH 7.0

CBP21 enzyme solution

Method

The reaction volume was 300 µl. The substrate suspension was continuously stirred with a magnetic stirrer in order to obtain consistent amounts when pipetting. Initial binding experiments were performed by using triplicates of the reaction mixtures that contained 2 mg/ml substrate and 100 µg/ml proteins in 50 mM sodium phosphate buffer, pH 7.0. The first reading was done without chitin in the cuvette. This had to be corrected for by subtracting the signal by a dilution factor; 60 µl chitin was added to the solution (after first reading), making a total of 300 µl reaction mixture. The reaction mixture was rotated vertically at 60 rpm at room temperature. At time points 5, 15, 45, 75, 105, 120, 150, 180, 240, 360 and 480 min, the substrate was spun down in a micro-centrifuge for 3 min at 13,000 rpm, and reduction of protein in the supernatant was determined by measuring absorption at 280 nm.

3.6 Activity assay

The CBP21 activity was measured indirect by measuring the effect CBP21 has on Chi-B. β-Chitin degradation was measured by determining the concentration of dimeres ($GlcNAc_2$) on a UHPLC (see section 1.18 for further details.

Sample materials and reagents

sample volume was set to 100 µL

β -chitin 2 mg/ml

CBP21 0.1 µM

Chi-B 0.5 µM

20 mM Tris- HCl pH8

Ascorbic acid 1mM

Stop solution: 100 µL acetonitrile (ACN)

Control:

The controls consisted of 20 mM tris-HCl pH8, 1 mM glutathione and β-chitin 2mg/ml. There were also three parallels of the sample material.

Instrumentation

Agilent 1290 Infinity UHPLC system

Software ChemStation rev. B.04.02 chromatography software was used to collect, integrate and analyze chromatograms

Column:

Waters UPLC BEH Aquity amide column.

Method

Triplicates with 100 µl sample material containing the enzyme and substrate was incubated at 37 °C and 1000 rpm in an Eppendorf shaker. The addition of stop solution to the sample was carried out after 30, 60 and 90 minutes. As stop solution, 100 µL acetonitrile was used.

The samples were frozen down at -24 °C until analysis. When analyzing the samples, they were thawed and then centrifuged at maximum speed for 5 minutes. Samples were pipetted into the appropriate HPLC vials, carefully not to contaminate samples with chitin.

The test volume on the instrument was set to 5 µL and the auto sampler was set to 10 °C, to avoid evaporation of ACN. Separation of dimeres occurred at a column temperature of 30°C with a flow rate of 0.4 ml/min and absorption reading at 205 nm.

The first big top is a waste top. The dimeres appeared as a small peak on the chromatogram after approximate one minute, while the tetrameres appeared after approximate 2 minutes, like two tops or one top with a “shoulder”.

4 Results

4.1 Studies on the binding of CBP21 to crystalline β-chitin

Binding studies were performed as described in (Vaaje-Kolstad et al. 2005b); se section 3.5.1 for more details. They were performed using β-chitin from squid pen as substrate and purified CBP21 wild type as enzyme. The binding of CBP21 was measured indirect by measuring reduction of the protein concentration in the supernatant at different time points, after incubation with β-chitin at room temperature. In an alternative approach, attempts were made to develop a new type of binding assay based on using fluorescence signals. The goal of this work was to develop the fluorescence assay; the UV work, that had been published previously, was done to check that the conditions for binding were okay.

4.1.1 Using UV to assay β-chitin binding

Figure 4.1 shows the binding of CBP21 to β-chitin over time. Clear binding is observed, which increases over time, with approximately 40 % of the protein being bound after incubation for 280 minutes. This implies binding of about 20 µg CBP21 per milligram of chitin.

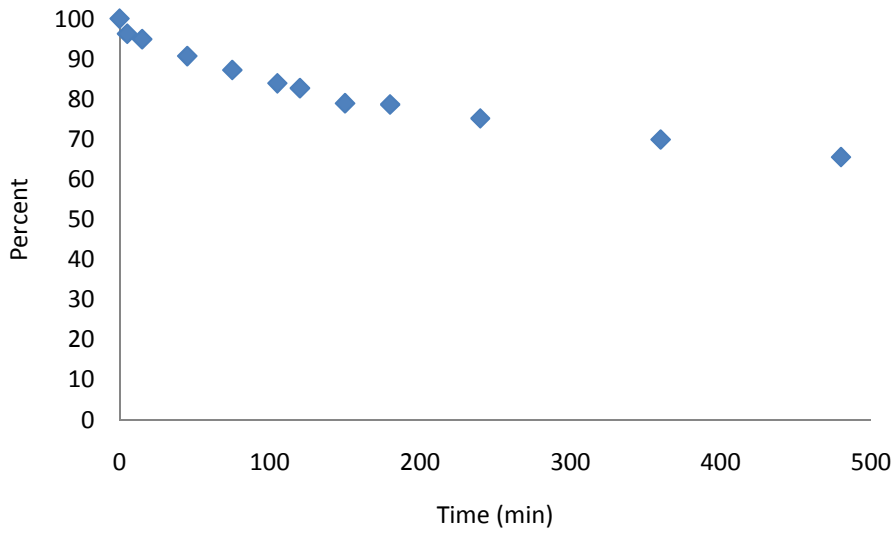

Figure 4.1: **Binding of CBP21 to β-chitin**. The data shown are the average of three parallels from the same run (average CV=9.7% measured from the absorbance raw data). The experiments were conducted using 100 µg/ml purified CBP21 and 2 mg/ml β-chitin in 50 mM sodium phosphate buffer, pH 7. Reduction of the protein concentration in the supernatant was determined by measuring absorption at 280 nm. The absorption of 0.1 mg/ml CBP21 solution without substrate incubated under the same conditions was used for determining the 100 % value.

4.1.2 Using fluorescence to assay β-chitin binding

Attempts were made to develop a more efficient and sensitive binding assay based on protein fluorescence instead of UV absorption. Binding reactions were set up by mixing β-chitin, CBP21 and buffer in a quartz-cuvette, followed by measuring the fluorescence signal over time. The expectation was that the fluorescence signal would decrease as the protein binds to the substrate. The idea was to use this assay for testing the effects of compounds such as metals and reductants, which are known to affect CBM33 activity (see section), on binding. Binding assays were performed with β-chitin as substrate in 50 mM sodium phosphate buffer pH7.

As a first step in developing this assay, the ratio between the protein concentration and the fluorescence signal was evaluated, as shown in figure 4.2. This experiment showed good linearity, indicating that it indeed would be possible to reliably measure protein concentration by using fluorescence. However, when binding assays were done it turned out that it was not possible to obtain reproducible results. As shown by figures 4.3 and 4.4, several problems occurred at the same time. Firstly, there were huge differences between identical experiments. Secondly, CBP 21 also seemed to disappear from solution in the absence of substrate, often to the same extents and at the same rates as in the presence of substrate (figure 4.4). Thirdly, the fluorescence signal at t=0, which in principle should be similar, showed large differences. Many attempts were made to optimize this experimental set-up, without success.

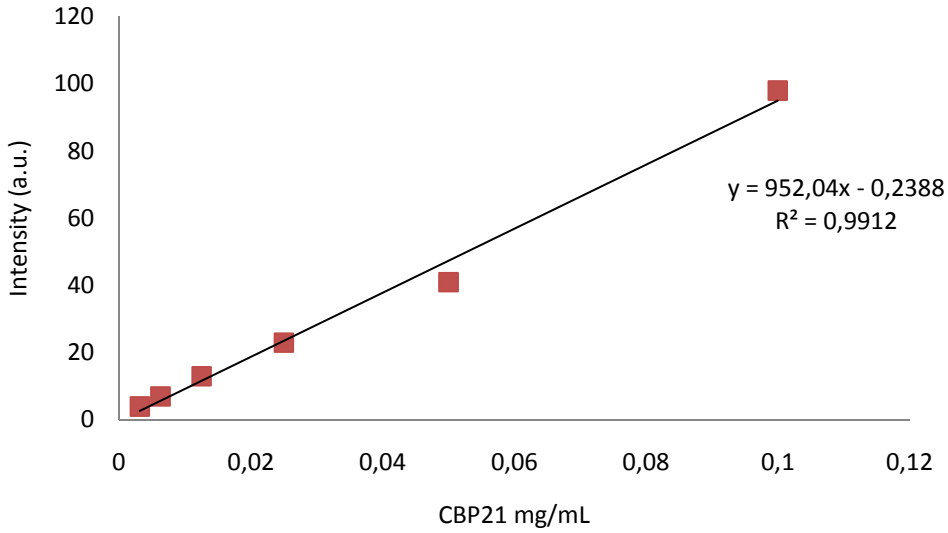

Figure 4.2: Ratio between the fluorescence signal and CBP21 concentration. The graph shows **f**luorescence intensity measured at excitation 295 nm and emission 345 nm on six different concentrations of purified wild type CBP21 in 50 mM potassium phosphate buffer pH7.

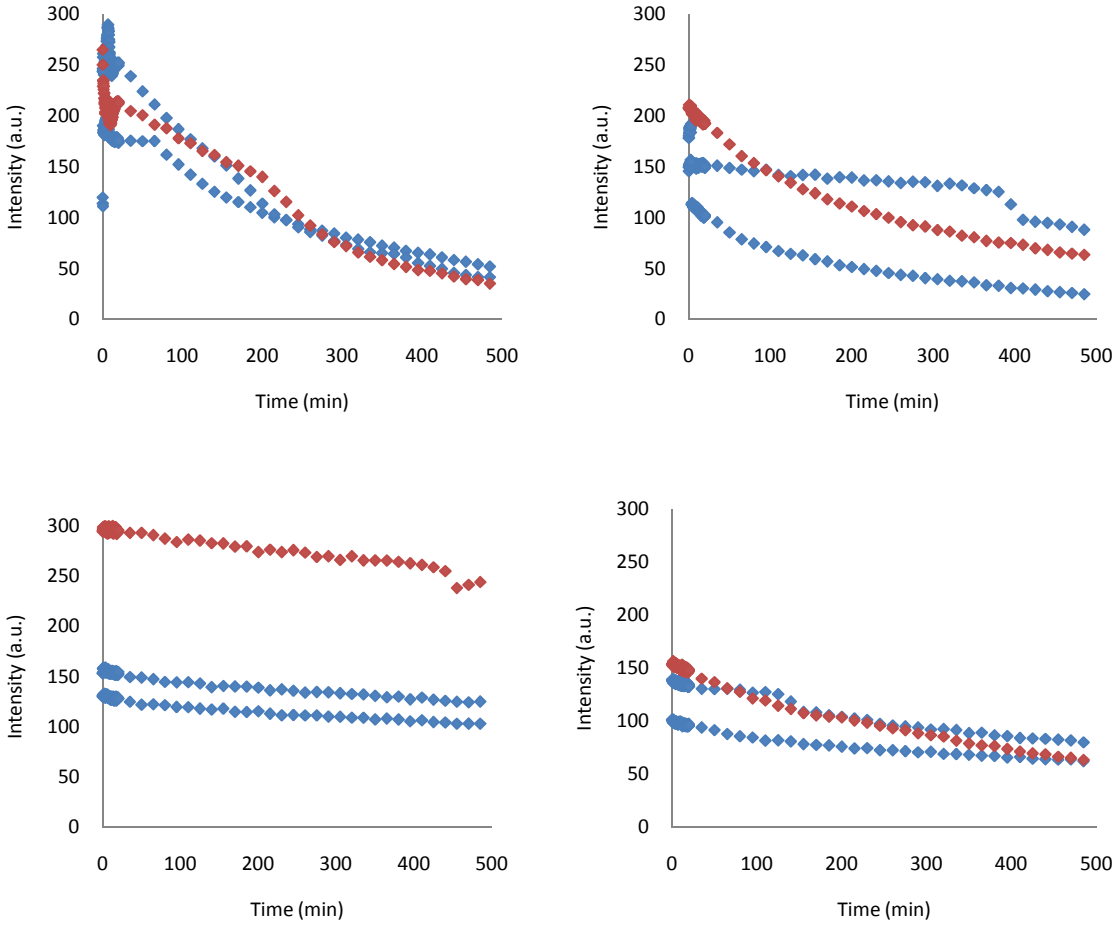

Figure 4.3: **Binding of CBP21 to β-chitin assayed using fluorescence.** The graph shows sets of experiments carried out on the same day. The reactions were set up as follows: 100 µg/ml purified CBP21 and 2 mg/ml β-chitin in 50 mM potassium phosphate buffer pH 7 (blue diamonds), or, in the control reaction with no substrate, 100 µg/ml purified CBP21 in the same buffer (red diamonds). Four different experiments are shown. The figures show large variations in quantum yield between the four different experiments, and within two parallels from the same experiments.

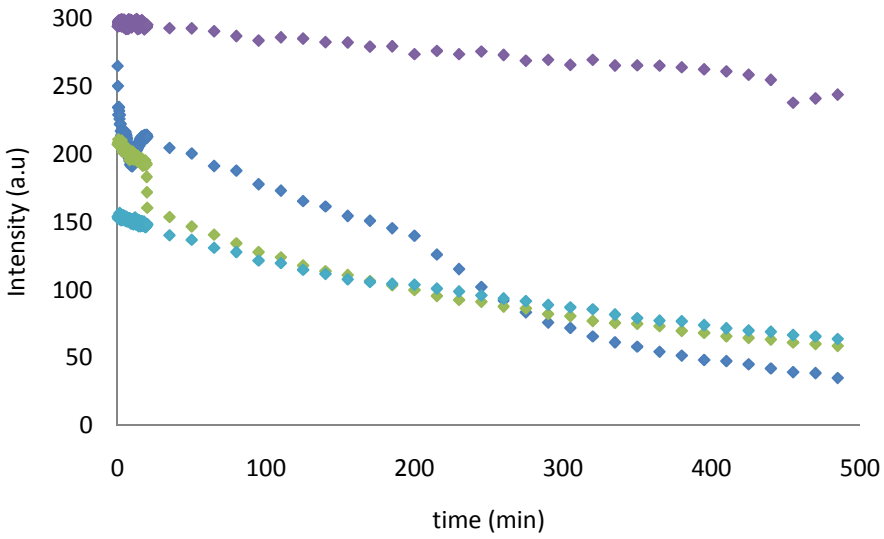

Figure 4.4: Comparison of the control reactions shown in Figure 4.3. The figure shows the control samples (100 µg/ml CBP21 in 50mM sodium phosphate buffer pH7) from the four different binding experiments shown in figure 4.3. The figure shows the decrease of the fluorescent signal with time in the control samples despite the absence of substrate. The decrease of the control signal was in some cases in the same size range as the decrease in the signal of the samples with substrate (Figure 4.3).

Of the possible explanations for these results; see section 5.1 for further discussion, possible effects of bleaching were tested in detail (figure 4.5). These results clearly showed that the decrease in signal is not due to photo bleaching from the UV radiation used for excitation.

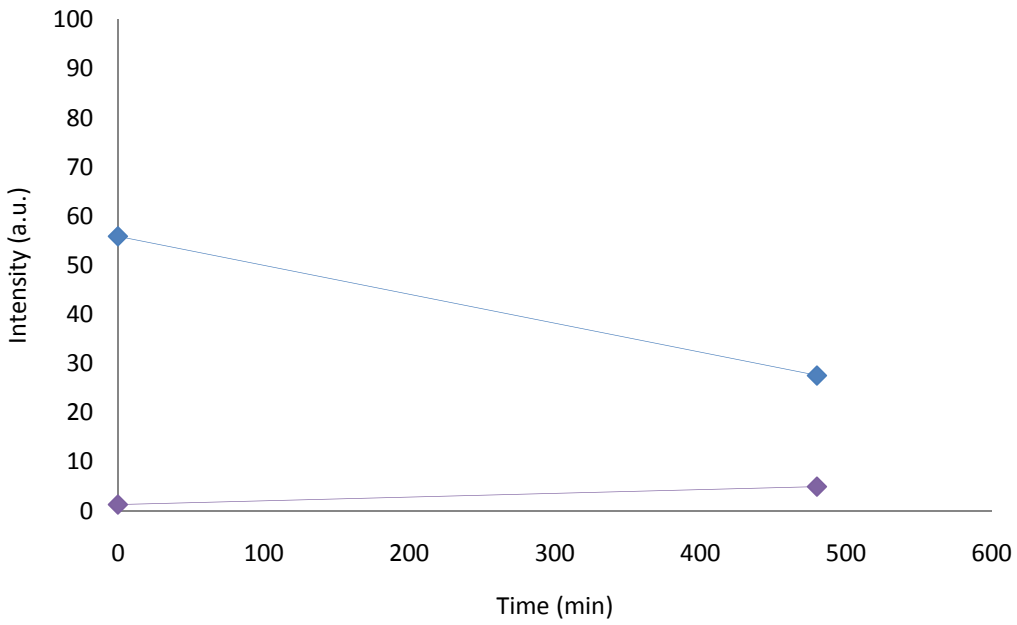

Figure 4.5: The control of bleaching. The figure shows control samples (100 µg/ml CBP21 in 50 mM sodium phosphate buffer pH7) on bleaching (blue line), and a control with only buffer (purple line) were examined to see if the fluorescence signal had the same intensity after incubating in the dark for 480 minutes (the duration of the binding experiments).

4.2 Design and production of mutants

In addition to the two wild-type CBM33 proteins, several mutated variants of CBP21 were included in this study. The basis of the mutant design was the three-dimensional structure of CBP21 (Vaaje-Kolstad 2005a, pdbid: 2bem). To enhance the thermo-stability of CBP21 four mutants (A130P, G73A and A155P) were generated, in addition we used the mutant Q161A, previously generated by Vaaje-Kolstad et.al (2005b). The mutation strategy that we chose was entropic stabilization (Xxx → Pro, Gly → Xxx). These mutations are presumes to restrict the degrees of freedom of the unfolded protein and so decrease the entropy of unfolding (see 1.16.1). To locate possible mutations we evaluated all residues in CBP21 against a large alignment of the CBM33 family and an alignment of four CBM33 proteins from thermostabile-organisms (figure 4.6). We also used the automated proline predictor SUGPRO, in the computer program WATHIF (Vriend, 1990). SUGPRO suggests possible mutations, and can give a good starting point for the evaluation of a possible mutation.

(Mutated CBP21 variants were generated, produced and purified as described in section 3.1, 3.2 and 3.3. Generally, the mutation procedure worked well, although one of the planned four mutants never was obtained. The mutant proteins were produced at the same levels and could be effectively purified by the same methods as the wild-type enzyme.

Considerations used in the evaluation of candidate sites for mutation.

- That the site was relatively solvent exposed. Candidates in the interior of the protein were discarded because of the risk that a mutation here would destabilize the 3D structure of CBP21.
- That the replaced residue did not participate in hydrogen-bonding, hydrophobic or electrostatic interactions with residues that are known to be important to the protein. If the mutation would change interactions with residues of unknown importance, we made a subjective evaluation of strength and importance of these against other factors that counted for the mutation (for example if the residue in question appeared in the alignment of the CBM33 family).
- That none of the atoms in the new residues was too close to other residues in the protein (no bumps created). The position of the new residues was decided based on suggestions from the rotamer search incorporated in PyMol.
- The level of conservation. All candidate sites were evaluated against the two alignments (the alignment of the CBM33's from thermo-stable organisms and the Pfam seed alignment)

Mutated CBP21 variants were generated, produced and purified as described in section 3.1, 3.2 and 3.3. Generally, the mutation procedure worked well, although one of the planned four mutants never was obtained. The mutant proteins were produced at the same levels and could be effectively purified by the same methods as the wild-type enzyme.

Q161A (Vaaje-Kolstad et al., 2005b) was designed because it could possibly reduce aggregation. This mutation was not guided by general principles of protein stability as this mutation would increase the entropy of unfolding (see section 1.16). The information contained in the sequence alignment is shown in figure 4.6. Gln161 plays a major role in the interactions between tightly packed CBP21 monomers in CBP21 crystals. Since it is possible that similar interactions may promote aggregation, the Q161A mutation could perhaps affect this process.

The three other mutations, A130P, G73A and A155P, could all lead to entropic stabilization, as explained in section 1.16. The sequence alignment used was from ClustalW2 (figure 4.6), the mutations were measured in PyMOL visualization program to look at distances to other residues.

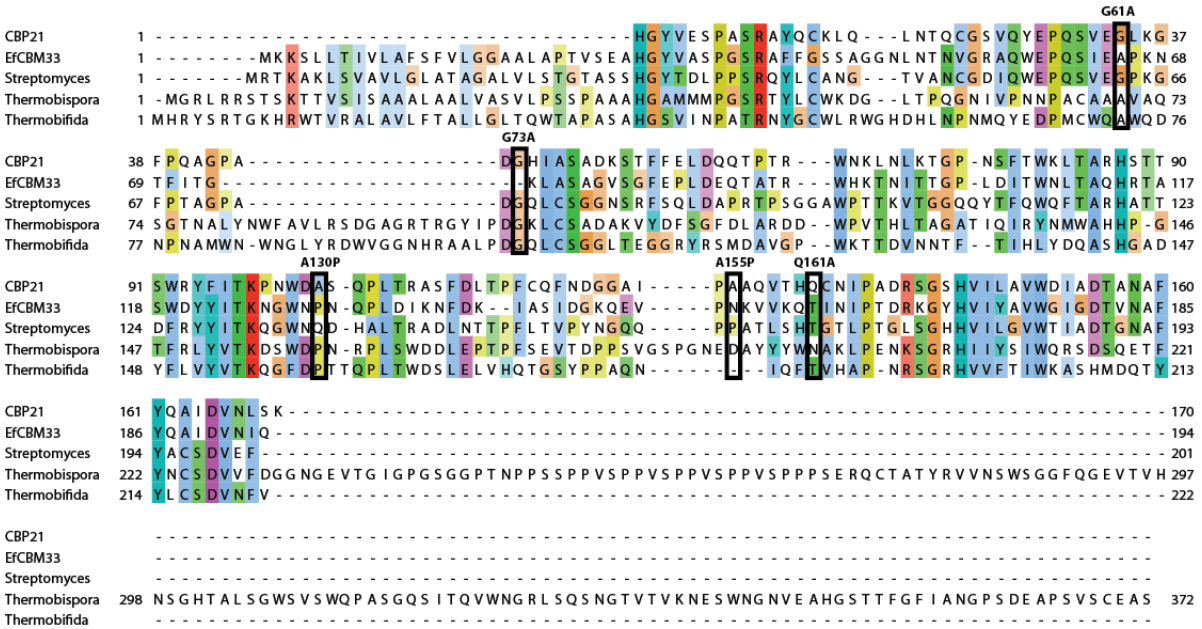

Figure 4.6: Sequence alignment of CBP21 and four CBM33 proteins. Mutations made in CBP21 from this alignment were G73A, A155P and A130P. The colors shown represent properties of the amino acid. The sequence alignment was made whit ClustalW2 (Larkin et al. 2007).

4.3 Re-folding test

Initial studies of the effect of heating on CBP21 and EfCBM33 showed that heating led to protein aggregation. Re-folding tests were performed for the two wild-type proteins and the A161Q mutant of CBP21 that had been specifically designed to reduce aggregation, to see if the aggregates that formed after heating to 80-90 °C would dissolve again upon cooling. Various experiments were conducted (figures 4.6-4.9) where parameters such as the protein tested, the heating rate, the cooling rate and cooling point were varied. The result clearly shows that all tested proteins aggregated under all tested conditions and that aggregation could not be reversed by cooling.

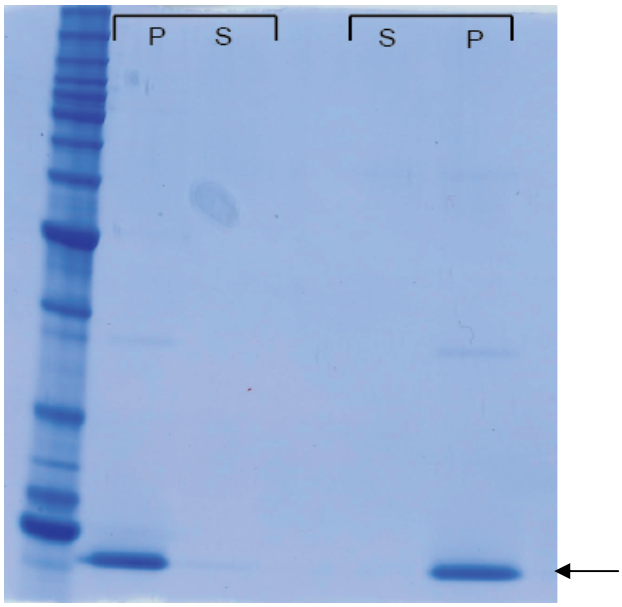

Figure 4.7: Refolding of EfCBM33. SDS-PAGE analysis of supernatant (S) and Pellet (P) after cooling of 2 µM EfCBM33 in 20 mM TrisHCl pH 8 from 80 °C to 20 °C at 5 °C/min (left) and after cooling from 80 °C to 0°C at 1°C/min (right). The marker (left lane) is Benchmark protein ladder from InVitrogen. The arrow indicated the position of the EfCBM33 band

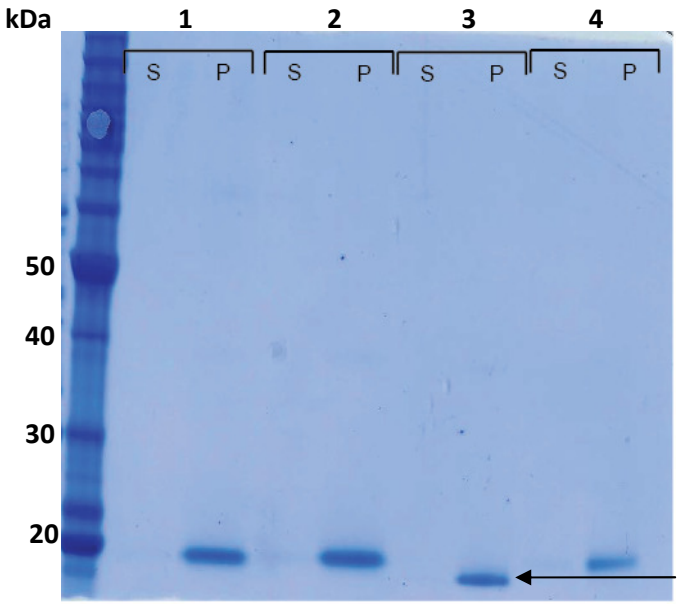

Figure 4.8: Refolding of EfCBM33, CBP21 wt and the CBP21 mutant Q161A (the mutant that was made to prevent aggregation). SDS-PAGE analysis of, **1:** CBP21 wt Supernatant (S) and Pellet (P) from a sample taken at 80 °C after heating from 25 °C to 80 °C at 5 °C/min. **2:** CBP21 wt Pellet (P) and supernatant (S) after cooling from 80 °C to 20°C. **3**. EfCBM33 Pellet (P) and Supernatant (S) after heating from 25 °C to 80 °C at 5 °C/min. **4:** The CBP21 mutant Q161A, Pellet (P) and Supernatant (S), after cooling from 80 °C to 20 °C at 5°C/min. The protein concentration was 2µM in 20 mM TrisHCl pH 8 in all cases. The arrow indicates the position of the EfCBM33 band, while CBP21 mutant and wt are expected to be located at position 19 kDa

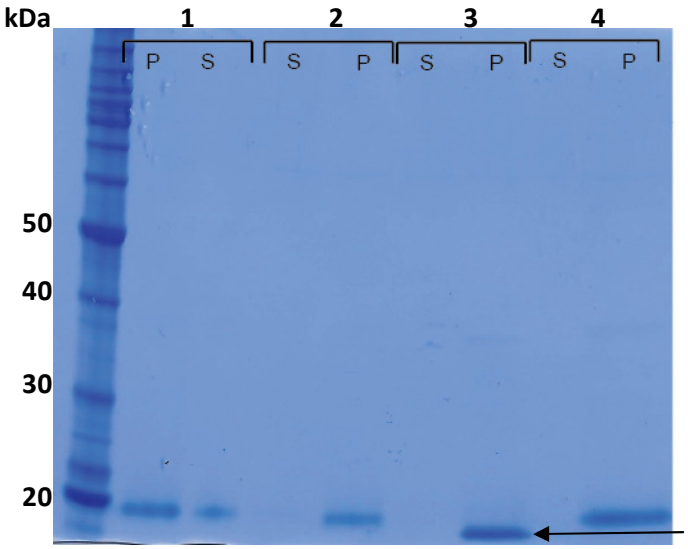

Figure 4.9: Refolding of EfCBM33 and the CBP21 mutant Q161A (a mutant that was made to prevent aggregation) SDS-PAGE analysis of **1:** CBP21 wt Supernatant (S) and Pellet (P) from a sample taken at 80 °C after heating from 20 °C to 80 °C at 1 °C/min. **2:** Q161A Pellet (P) and supernatant (S) sample taken at 80 °C after heating from 20 °C to 80°C. **3**. EfCBM33 Pellet (P) and Supernatant (S) sample taken at 80 °C after heating from 25 °C to 80 °C at 1 °C/min. **4:** The CBP21 wt, Pellet (P) and Supernatant (S), sample taken at 20 °C after cooling from 80 °C to 20 °C at 5°C/min. The protein concentration was 2µM in 20 mM TrisHCl pH 8 in all cases**.** The arrow indicates the position of the EfCBM33 band, while CBP21 mutant and wt are expected to be located at position 19 kDa. In well number three there seems to be some pollution from CBP21 w.t 80 °C protein pellet.

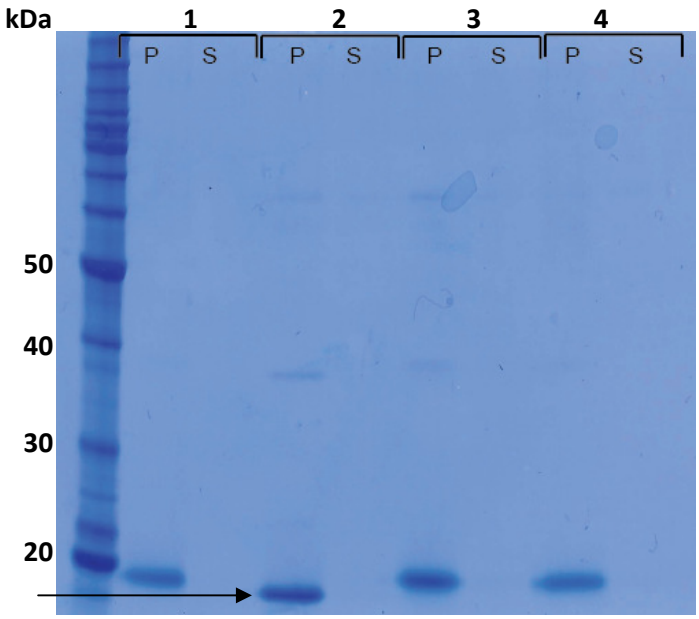

Figure 4.10: Refolding test of EfCBM33,CBP21 wt and CBP21 mutant Q161A (a mutant that was made to prevent aggregation) SDS-PAGE analysis of, **1:** Q161A Supernatant (S) and Pellet (P) from a sample taken at 20 °C after heating from 20 °C to 80 °C at 1 °C/min. **2:** EfCBM33 Pellet (P) and supernatant (S)sample taken at 20 C° after heating from 20 °C to 80°C at 1 °C/min. **3**. CBP21 wt Pellet (P) and Supernatant (S) sample taken at 0 °C after heating from 20 °C to 80 °C at 1 °C/min. **4:** The Q161A , Pellet (P) and Supernatant (S), sample taken at 0 °C after cooling from 80 °C to 20 °C at 5°C/min. The protein concentration was 2µM in 20 mM TrisHCl pH 8 in all cases**.** The arrow indicates the position of the EfCBM33 band, while CBP21 mutant and wt are expected to be located at position 19 kDa.

4.4 Thermo stability of CBP21 and EfCBM33

Thermo stability is one of the most important qualities of a protein and hence one of the protein properties that is often improved through protein engineering efforts. In this thesis intrinsic fluorescence and circular dichroism was used to assess the protein stability of CBP21 and EfCBM333. To improve the thermo-stability of CBP21, four mutants were made using intrinsic fluorescence in section 1.7.1 and 3.4.1

4.4.1 Circular dichroism (CD) measurements of the thermal-unfolding of CBP21 wild-type and EfCBM33

Since proteins are chiral objects, their secondary structure content can be measured quantitatively using circular dichroism. CD spectra may be divided into the far UV region (180-250nm), the near UV region (250-300nm), and the UV – vis region (300-700nm). Absorption in the far UV region gives us information about the secondary structure. CD may be used to measure unfolding, by monitoring secondary structure during heating. CD can also be used to study the presence of structure in before and after heating a protein, although aggregation may create some complications when analyzing heated samples because the proteins in solution starts to precipitate and thereby disappears from the solution. Fig. 4.14 shows CD spectra of CBP21 before and after heating. The figure clearly shows that heating causes loss of structure. Similar experiments were done for EfCBM33, with similar results (Fig. 4.15).

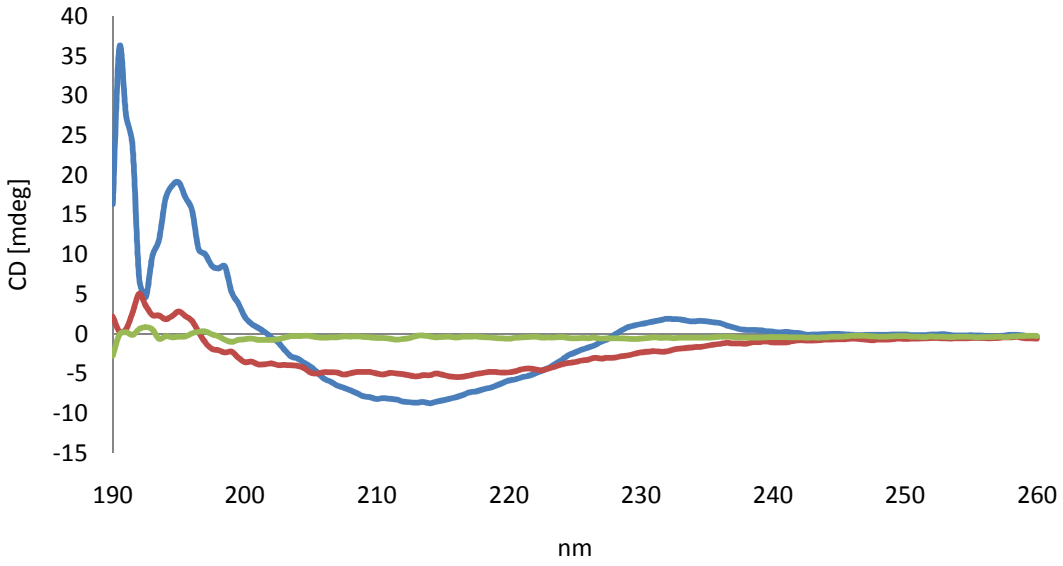

Figure 4.11: Circular dichroism scan of CBP21 wt. The figure shows the scan of 0.2 mg/ml CBP21 in 20 mM TrisHCl before (blue) and after (red) heating from25-80 °C. 20mM tris-HCl pH 8 was used as control (green) CD scans were performed from 190 nm to 260nm

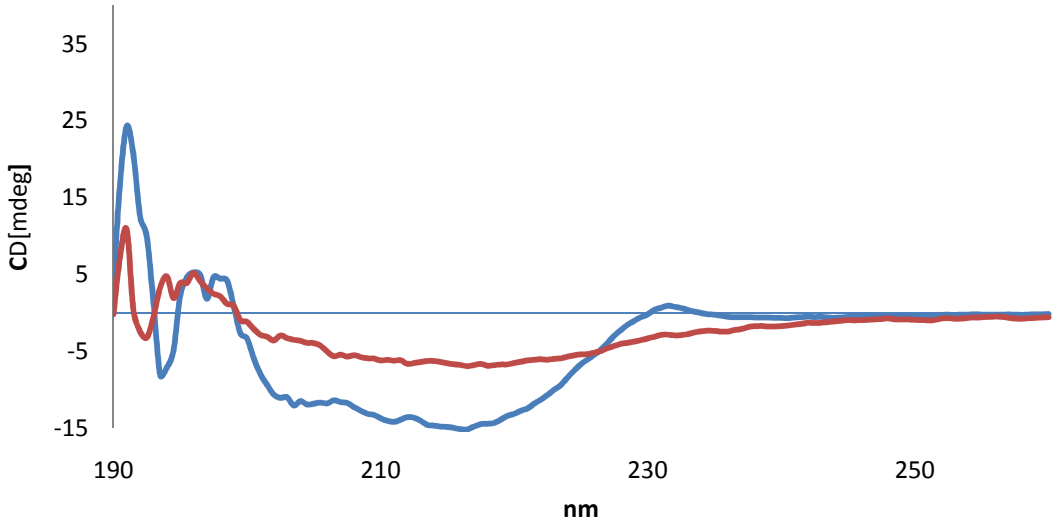

Figure 4.12: Circular dichroism scan of EfCBM33 The figure shows the scan of 0.2 mg/ml EfCBM33 in 20 mM TrisHCl before (blue) and after (red) heating from25-80 °C. 20mM. CD scans were performed from 190 nm to 260nm

In protein unfolding studies, unfolding is usually monitored by measuring the CD signal at 222nm which is indicative of helicity. CBM33 proteins have little helical structure and, accordingly, the spectrum of CBP21 (Fig. 4.14, red curve) showed little signal at 222 nm. For EfCBM33, a slightly stronger helical signal (at 222 nm) was observed (Fig. 4.15, blue curve) due to somewhat more helix structures in EfCBM33. Attempts were made to monitor unfolding in the CD spectrophotometer. The results, depicted in Fig. 4.16, show a clear transition in the 70 °C – 80 °C for EfCBM33, but not for CBP21. The CD apparatus also reports UV absorption signals and these signals (Fig. 4.17) showed a clear transition for both proteins, at approximately the same temperature.

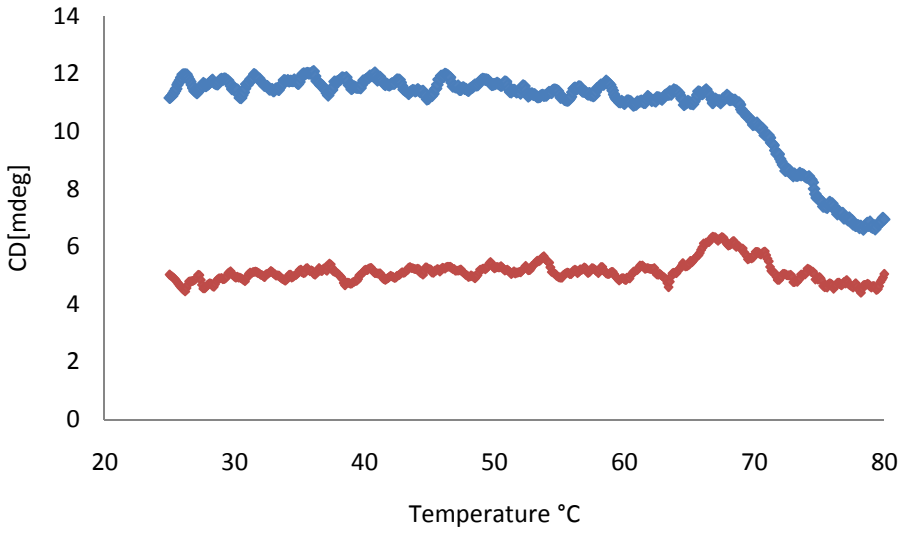

Figure 4.13: Temperature scan of CBP21 by measuring the CD signals at 222nm wt (0.2 mg/ml, red) and EfCBM33 (0.2 mg/ml, blue), in 20 mM TrisHCl. The size of the CD signals varied between the proteins. Shown here are the raw data from 25-80 °C. The heating rate was 1 °C/min

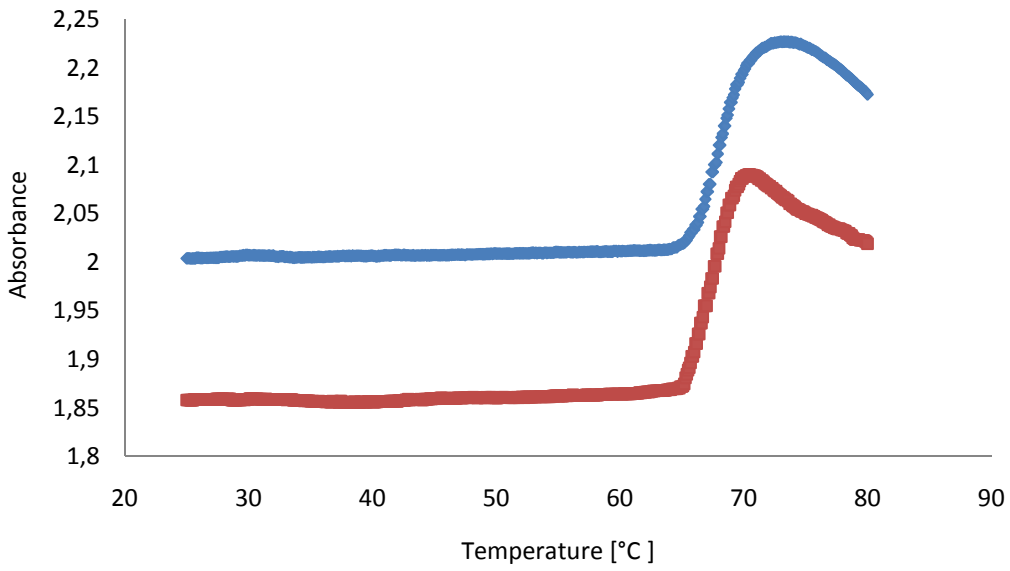

Figure 4.14: Temperature scan by measuring UV absorbtion from the Circular Dichroism experiments. In addition to the CD signals the CD instrument also report UV absorption signals. The figure shows the UV absorbtion from the same unfolding experiment as in figure 4.16 of CBP21 (red) and EfCBM33 (blue) both at 0.2 mg/ml. Absorbance was read at 222nm while heated from 25-80 °C 1°C/min. Shown here are the raw from 25-80 °C

Measuring CD signals to monitor unfolding of CBP21 and EfCBM33 did not give satisfying results and so CD measurements were replaced by a more optimal tool for this purpose by fluorescence measurements.

4.4.2 Fluorescence measurements of the thermal-unfolding of CBP21 wild-type, mutants and EfCBM33

Further studies in the effect of heating of CBP21 and EfCBM33 were done in a fluorescence spectrophotometer under varying parameters such as the change in the rate of temperature increase, the protein concentration and the presence of metals (section 3.4.1). In addition to the wt, four mutants of CBP21 were assayed for thermo-stability. The raw data from the fluorescent assay were converted to a sigmoid unfolding curve by calculating the apparent fraction of unfolded protein (apparent tm). When apparent Tm is 0 the protein is totally folded, and when apparent Tm is 1 the protein is totally unfolded. At the apparent melting temperature of the protein (apparent T_m) 50 % of the protein is folded and 50 % is unfolded, this correspond to a apparent Tm of 0.5 (Pace 1990). Apparent Tm is described by the following formula

$$\text{Apparent Tm} = \frac{(\text{Yf} - \text{Yobs})}{\text{Yf} - \text{Yu}}$$

Where Y_n= value of y for the native part of the curve, Y_{obs}= observed fluorescence signal, Y_d= value of y for the denatured part of the curve. From the apparent Tm versus Temperature curve the apparent melting temperature of the protein is estimated as the temperature at apparent Tm =0.5. Typical curves obtained using optimal settings (heating rate, protein concentration) are shown in figure 4.9 which gives an overview of the CBP21 variants tested in this study. More details are given below, in section 4.43-4.45.

The fluorescence assay was improved and developed by trying different wavelengths and concentrations as the proteins were exposed to temperatures ranging from 20-90 °C. This was done to see the temperature at which the proteins unfold and whether the proteins are able to refold or not. The proteins were incubated with metals to see if this would stabilize them to tolerate higher temperatures.

To obtain the results to produce figure 4.9, several parameters were tested, as described in section 3.4.1. One parameter was the heating rate, for which an experiment is shown in figure 4.10. The results show that CBP21 unfolds at a higher temperature when heating rate is increased from 1 °C/min to 5 °C/min. These results show that the protein is not in equilibrium between the folded and unfolded state.

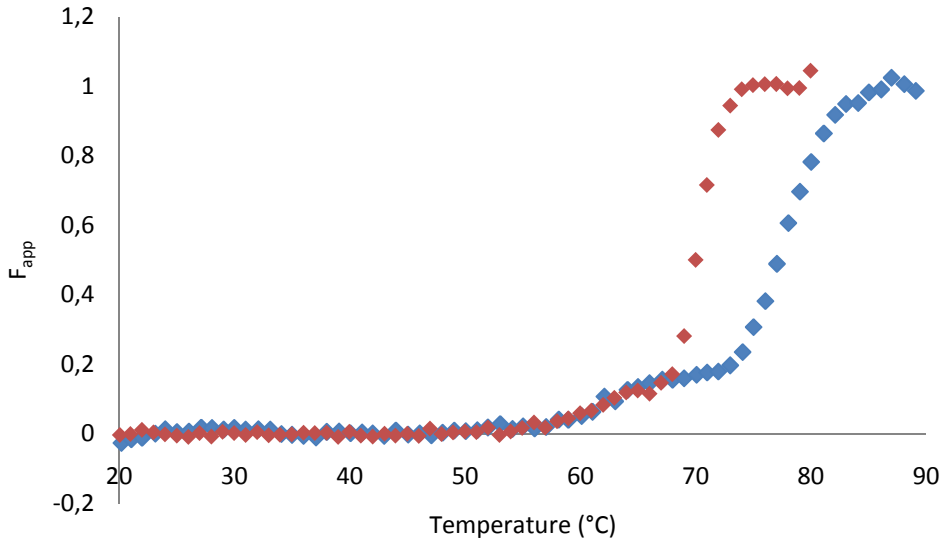

Figure 4.15: **The apparent melting temperature decreases when the heating rate increases.** The figure shows the unfolding of CBP21 wild-type (2µM) with a heating rate of 5 °C/min (blue squares) and 1 °C/min (red squares). When the heating rate increases the apparent Tm increases with approximately 5 °C. This indicates that the unfolding of CBP21 is a kinetic process.

Table 4.1: Apparent melting temperature of CBP21 wild-type, mutants and EfCBM33. The apparent Tm values are calculated from the average between two parallels in two different runs (four unfolding curves in total for each Tm value reported).

	1 °C/min, 2µM	5 °C/min, 5 µM	5 °C/min, 2µM
CBP21 wt	70.3 °C	75.0 °C	77.0 °C
Q161A	68.0 °C		
EfCBM33	72.0 °C		
A130P	72.5 °C		
G73A	64.8 °C		
A155P	70.6 °C		

4.4.3 EfCBM33 and CBP21 with and without DTT

To see if the disulphide bridges in CBP21 stabilize the protein, both CBP21 and EfCBM33 were incubated with DTT a disulphide destroyer (figure 4.11). These results show that the stability of CBP21 is dramatically decreased by 6.2 °C (table 4.2) and that the stability of EfCBM33 is not decreased to the same extent.

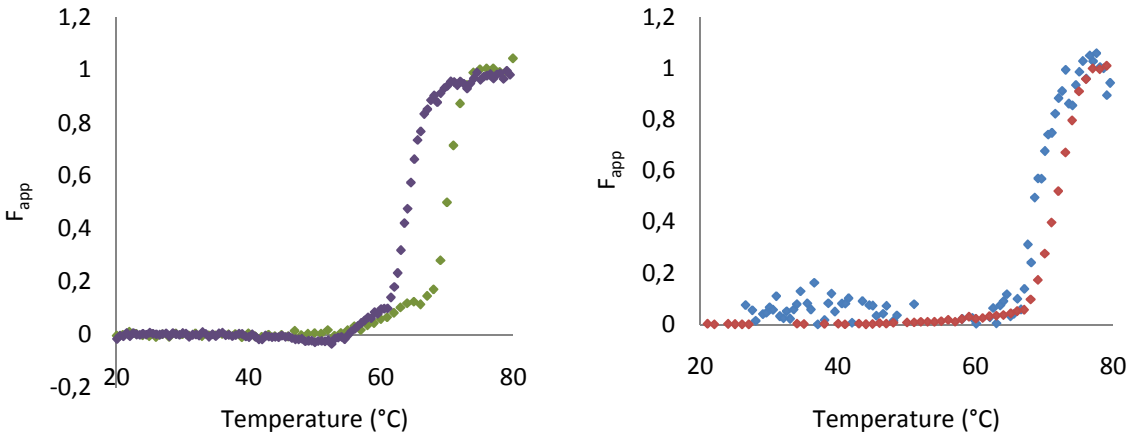

Figure 4.16: The effect of DTT on the unfolding of CBP21 and EfCBM33. At the left the effect of unfolding 2 µM EfCBM33 in 20 mM TrisHCl with (purple squares) and without (green squares) 2 mM DTT is shown. DTT decreases the apparent Tm of CBP21 with 6 °C. The panel at the right show the unfolding of 2 µM EfCBM33 with (blue squares) and without (red squares) DTT. The heating rate was set to 1 °C/min.

Table 4.2: Apparent melting temperature depends on DTT. The values reported are the average of two parallels from the same run. At the apparent melting temperature of the protein (apparent T_m) 50 % of the protein is folded and 50 % is unfolded, this correspond to a apparent Tm of 0.5

Mutant	Apparent T_m
CBP21 wt	70.3 °C
DTT CBP21 wt	64.1 °C
EfCBM33	72.0 °C
DTT EfCBM33	70.5 °C

The DTT experiment gives an interesting result, showing that disulphide bridges do stabilize the protein structure.

4.4.4 Effect of metal ions on CBP21 unfolding

Further, to look at the thermal-stability, CBP21 was incubated with $MgCl_2$, $CaCl_2$ and $ZnCl_2$ to see if this would stabilize CBP21 to tolerate higher temperatures (figure 4.12 4.13 and table 4.3). CBP21 was also incubated with EDTA (figure 4.12). The thermal-stability curve appeared unchanged when incubating with $CaCl_2$ and $MgCl_2$. $ZnCl_2$ showed to change the unfolding curve of CBP21. The shape of the unfolding curve of CBP21 shows a dose-response towards the addition of $ZnCl_2$. (figure …). This change was not necessarily in a stabilizing manner. EDTA is a metal binder that removes the divalent metal in CBP21 metal binding site. When EDTA is added to the unfolding reaction it seems that the unfolding of CBP21 changes from a two-state folding to a more complex folding behavior (the absence of metals seems to induce a "bump" in the unfolding). The change in the unfolding by adding EDTA shows that metals are important for the stability of CBP21 (figure4.12).

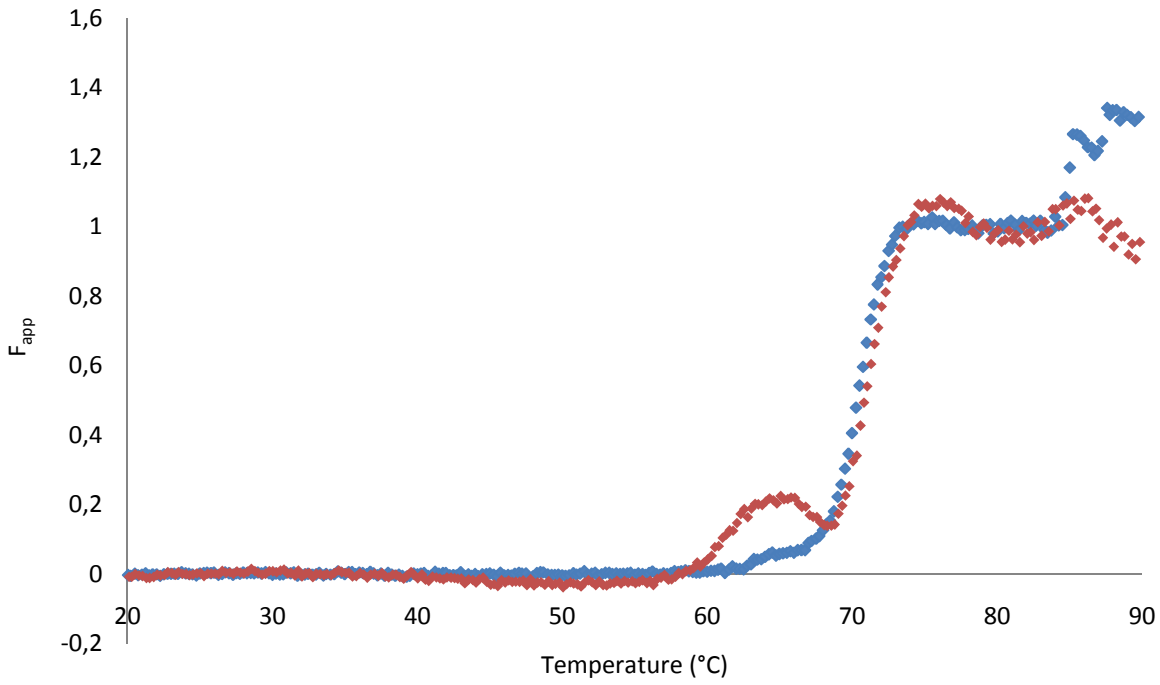

Figure 4.17: The shape of the unfolding curve of CBP21 depends on $ZnCl_2$ The unfolding of 2 µM CBP21 in 20 mM TrisHCl with 0.1 mM $ZnCl_2$ (blue squares) and 1mM EDTA (red squares). The heating rate was set to 1 °C/min.

Tabel 4.3: The dependence of the apparent melting temperature of CBP21 wt on divalent metals. The apparent Tms are calculated from the average between two parallels from one run. At the apparent melting temperature of the protein (apparent T_m) 50 % of the protein is folded and 50 % is unfolded, this correspond to a apparent Tm of 0.5

Divalent metal	Apparent T_m
$MgCl_2$	70.5 °C
$CaCl_2$	70.6 °C
$ZnCl_2$	69.1 °C
EDTA second unfolding	71.0 °C
EDTA first unfolding	61.1 °C[1]

1) The apparent Tm was calculated from the first unfolding of the apparent two state folding curve of CBP21 with EDTA added (Figure 4.12).

4.4.5 Dose response curve of the addition of $ZnCl_2$ in CBP21 unfolding

A dose response was performed due to the change in the unfolding curve when adding 0.1 mM $ZnCl_2$. The shape of the unfolding curves in the dose response assay shows that CBP21 shows a dose-response towards the addition of $ZnCl_2$.

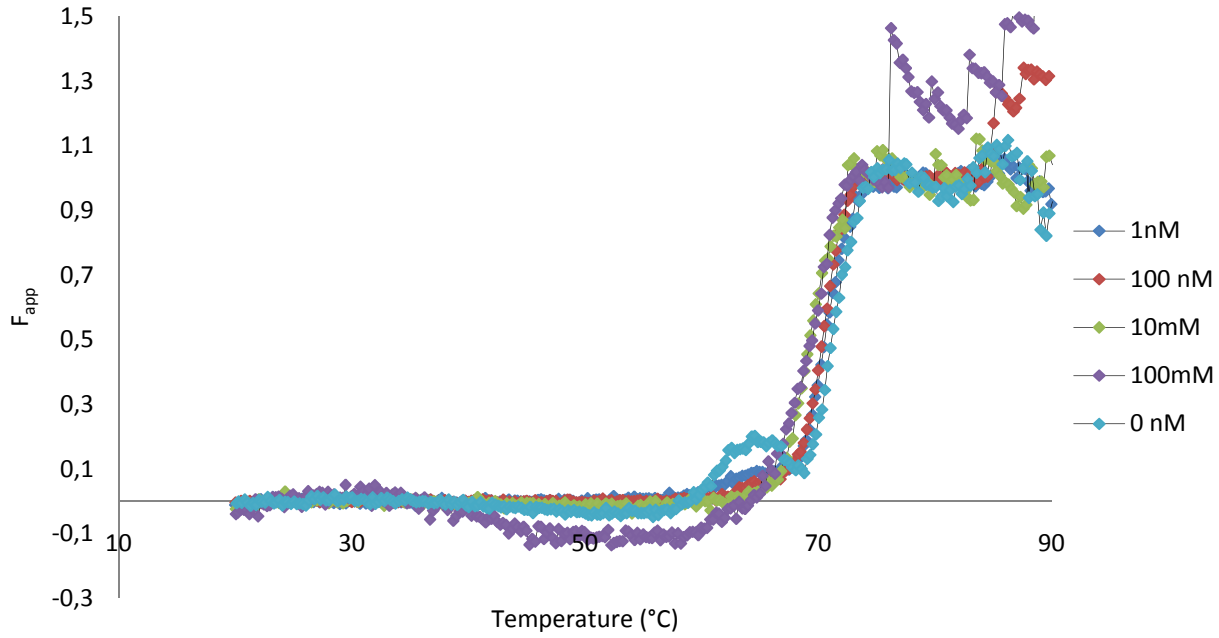

Figure 4.18: **The shape of the unfolding curve of CBP21 shows a dose-response towards the addition of $ZnCl_2$.** Different concentrations of ZnCl2 was added to the unfolding of 2 µM CBP21 wt in 20 mM TrisHCl. The heating rate was set to 1 °C/min. The 0 nM reaction mixture contains no metals and is added 1mM EDTA

4.4.6 Stability of designed CBP21 mutants

In the final part of the study, attempts were made to create more stabile CBP21 variants by introducing designed single site entropic mutations that are thought to make the enzyme structure more rigid. Of three designed entropic mutations, G73A, A130P and A155P one variant (A130P) led to a 2.2 °C increase in the apparent Tm. CBP21 A130P is the first ever reported thermo-stabile mutant of CBM33, and here one can see the thermal-optimization of the CBP21 variant A130P (purple diamonds)

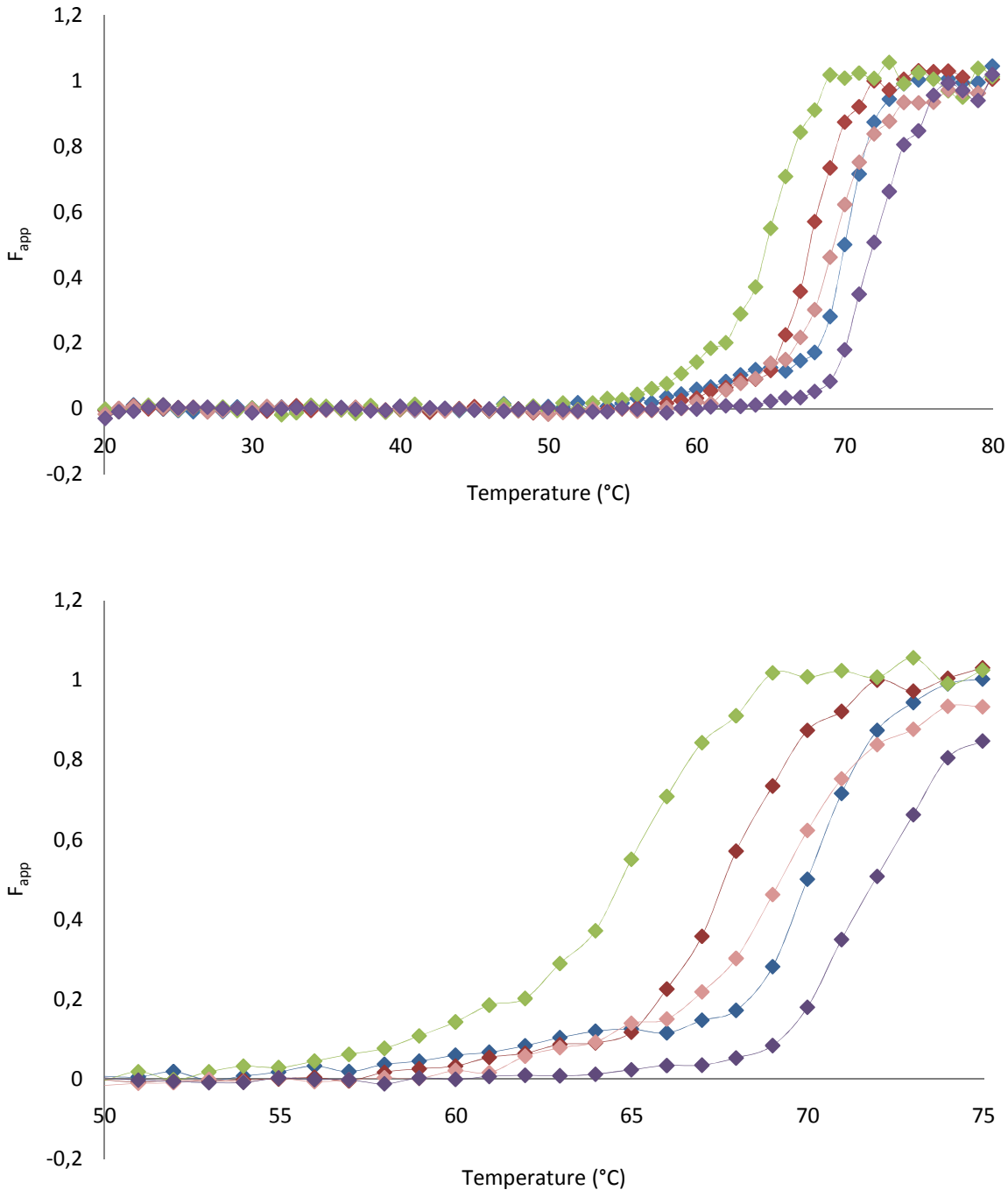

Figure 4.19: Thermo-stability of CBP21 wt and mutants. The upper panel shows the unfolding of CBP21 wt and mutants (all at 2µM in20 mM Tris pH 8); wild type (blue squares), Q161A (red squares),

G73A (green squares), A155P (pink squares) and A130P (purple squares). The heating rate was set to 1 °C/min. In the lower panel the curve is shown in more detail between 50-75 °C. The conditions used here were the result of lots of testing of various parameters, as described in previous sections. Here one

4.4.7 Effect of temperature on the activity of CBP21

To get a first glimpse of the temperature-dependency of CBP21 activity, two experiments were carried out, the results of which are shown in Fig. 4.19. Panel shows that CBP21 boosts the activity of a chitinase, Chi-B, at 50 °C, whereas panel b shows that the activity of CBP21 rapidly decreases at 70 °C. This is in accordance with the observations from the stability measurements which indicate that CBP21 unfolds around 70 °C.

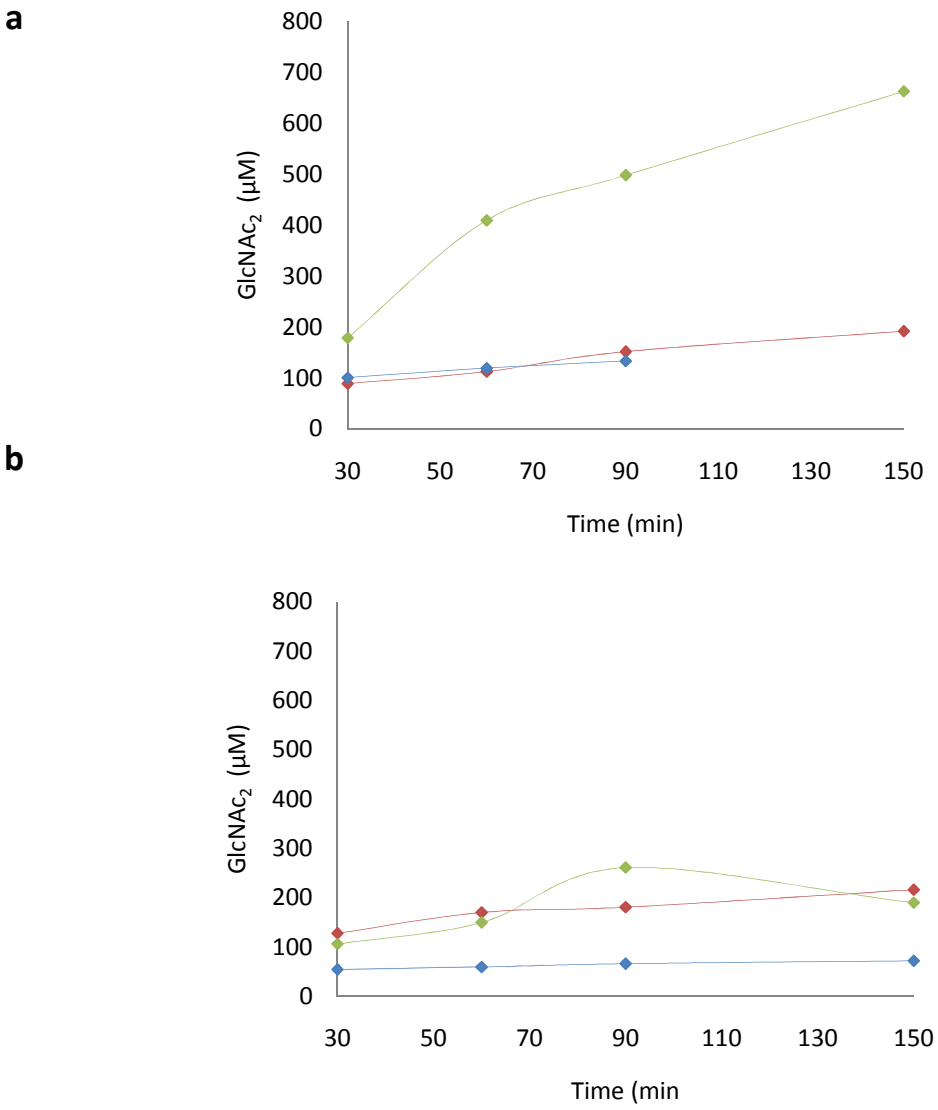

Figure 4.20: **Activity analysis of CBP21 on β-chitin.** 2 mg/ml β-chitin was degraded by Chi-B (0.5µM) in the presence or absence of CBP21 (0.1 µM) and ascorbic acid (1mM) in Tris-HCl buffer pH8 at 50 °C (panel a) or 70 °C (panel b). Colour coding: blue, Chi-B; red, Chi-B and ascorbic acid (red squares); green, Chi-B, CBP21 & ascorbic acid. Enzyme efficiency was assessed by measuring the release of chitobiose from chitin (Y-axis). Curve (a) with an average standard deviation of (SD) = 61.8 µM and a CV= 12 % between two sample parallels in the same run (first reading not included). Curve (b) with an average SD= 28.6µM and a CV= 13 % between two sample parallels in the same run.

4 Discussion

4.1 Assay on CBP21 binding to β-chitin

The first binding experiments were done by measuring protein concentrations using UV absorption at 280 nm, with CBP21 wild type and β-chitin. Similar experiments were also done by Vaaje-Kolstad et.al in 2005 (Vaaje-Kolstad et al. 2005b). After 100 minutes of incubation at room temperature, 16 % of the protein was bound to the substrate (figure 4.1). This percentage was considerably lower than previously achieved by Vaaje-Kolstad et.al in 2005b, (where about 60 % of the protein was bound after 100 minutes). The main reason for this difference is probably because of differences in the substrate that is used. In the paper by Vaaje-Kolstad et.al 2005b they used ultra small-chitin particles (β-chitin nanowhiskers) as opposed to the somewhat larger chitin flakes used in the experiments described in this thesis, which again shows the importance of having a good substrate to the enzyme. Also, these experiments were done on one protein batch. It could be beneficial to change protein batch of purified protein as it often turns out to be great variations in one protein batch of purified protein to the other.

It could also be that the reproduction of the binding assay was somewhat different compared to the preparation of point zero. In the experiments of this thesis, the zero sample was made by adding β-chitin to the cuvette after the first reading, which gives an absorbance signal that needed to be corrected for by a dilution error. Theoretically the absorbance of the zero-sample could be higher (if the absorbance of free protein at A280 is influenced by the addition of substrate), but this effect cannot explain all the difference between the binding curve in this experiment and the curve by Vaaje-Kolstad et al. since the slow decrease of the binding curve continues also after 5 minutes. The experiment was repeated several times, all repetitions gave the same shape of the curve, which further indicates that CBP21 has a different affinity to the substrate used in this thesis than the substrate used by Vaaje-Kolstad et al.

Assaying CBP21 binding on a UV spectrophotometer with the method developed by Vaaje-Kolstad is quite laborious and because of that we wanted to develop a method based on continuous measurements in a fluorescence spectrophotometer. The idea was to measure the binding of the protein to the substrate by continuously measuring the loss of protein from the solution. CBP21 was supposed to bind to the substrate and as a result of the binding disappear from solution thereby giving a decline in fluorescence-intensity in the fluorescence-spectrophotometer.

Looking at the effects of different parameters such as different concentrations of both enzyme and substrate one could see in figure 4.3 and 4.4 that in some cases the decline in the absorbance in the control with only CBP21 was higher than in the actual enzyme-substrate mixture. The reason for this is not clear. It could be photo bleaching of signal (loss of fluorescence signal over time), but figure 4.5 indicates that this is not the case (see below). The decline in absorbance of the sample with chitin and CBP21 could come from that the substrate lowers the signal from the enzyme in some way. It could also be that the sodium phosphate buffer at pH 7 was not suitable for these kinds of experiments, although this buffer has been used in tryptophan fluorescence assays found in literature (Bruderlein & Bernstein 1979; Haifeng et al. 2008). The reduction in control sample signals was the main reason for discarding the procedure.

A test was performed to see if there was any bleaching of the fluorescent signal (figure 4.5). This was done by placing the cuvette containing CBP21 wild-type in the dark for 8 hours after the first reading. The test showed that there is no photo-bleaching of the fluorophore as the signal was reduced by a factor two after incubation in the dark, which is roughly the same as is seen in the other binding assays performed in the fluorescence spectrophotometer (figure 4.3).

4.2 CBP21 and EfCBM33 unfold irreversibly

Proteins are able to re-fold spontaneously after unfolding, as long as there is equilibrium between the folded, functional state and the unfolded or partially unfolded state.

To see if this was the case for CBP21 and EfCBM33 a re-folding test was performed (figures 4.7-4.10). After seeing that the top of the unfolding curve was at approximately 80 °C when the heating rate was set to 5 °C/min, we wanted to see if we could get refolding if reduced the temperature from 90 °C to 80 °C, at the peak of the unfolding curve. Both proteins as well as engineered mutants of CBP21 aggregated when heated to 80°C and the re-folding tests showed that they did not refold upon cooling. This indicates that there is no equilibrium between the folded and unfolded state when heated to 80°C neither at 1 °C/min nor at 5 °C/min.

This test does not say anything about when the proteins aggregate, but only shows that all the protein are aggregated at 80 °C and that they don't refold when they are cooled down 1 °C/min or at 5 °C/min, which indicates an irreversible unfolding process. Also, if there is an irreversible unfolding process, one should expect that apparent Tm increases with increased heating rate, which was actually observed under these studies (see section 4.15)

4.3 Thermo-stability studies of CBP21 and EfCBM33

Higher temperatures give higher reaction rates and are thus beneficial for the degradation of the crystalline substrate by CBM33 enzymes. In this thesis we have increased the thermo-stability of CBP21 by entropic stabilization and we have looked at the importance of disulphide bridges for stability of this type of enzymes. The CBP21 and EfCBM33 have fluorescent tryptophans and tyrosines on the inside of the proteins. This is used as a measure of unfolding as these aromatic amino acids show a change in fluorescence during unfolding. Also, circular dichroism experiments were performed to haven an alternative for unfolding measurements based on intrinsic fluorescence. Since proteins are chiral objects, their secondary structure content can be measured quantitatively by using circular dichroism. The problem is that the CD signal indicative of the presence of alpha-helices (at 222nm) is the most robust parameter for structure while CBM33 proteins have very low helical contents.

4.3.1 Using Circular dichroism to assay thermo-stability

While the CD signals at 222 nm from EfCBM33 showed a clear transition during heating, no such transitin was observed for CBP21 (figure 4.13, 4.14). Thus, the use of CD did not allow comparison of the two wild-type proteins or comparison of CBP21 with its engineered mutants. When measuring CD signals a UV spectrum is also measured at the same wavelength and the UV spectra at 222 nm were easier to interpret. Based on UV signals, it looked as if CBP21 and EfCBM33 have the same stability, with an unfolding transition around 65 °C. This reinforces the results from the fluorescence experiments, which indicates that the stabilities of the two proteins were similar despite the presence of disulfide bridges in CBP21 only.

The CD scans from 190nm to 260 nm (figure 4.11, 4.12) shows that both CBP21 wt and EfCBM33 have lost most of their structure after heating, which reinforces the results from the fluorescence refolding assay that the proteins do not re-fold after heating.

4.3.2 Thermo-stability using different heating rates

Protein stability can be divided into two categories, thermodynamic stability and kinetic stability. Thermodynamic stability is characterized by a low amount of unfolded and partially unfolded protein being in equilibrium with the native, functional protein (Sanchez-Ruiz 2010).

Kinetic stability is characterized by a high free energy barrier of the protein which separates the native state from the non functional form. In kinetic stability there is no equilibrium between folded and unfolded form; it is the energy barrier that keeps the protein stabile for a sufficient amount of time. This energy barrier can be affected by mutations such as entropic stabilization, making the energy barrier of the protein even higher (Sanchez-Ruiz 2010).

The unfolding assay done in this study revealed that CBP21 unfolded at a higher temperature when the heating rate was at 5 °C/min (figure 4.15, table 4.1) compared to 1 °C/min. It was also discovered that the unfolding process was much more unpredictable when the heating rate occurred at 5 °C/min (table 4.1), which also gave an indication that the proteins were not in equilibrium between folded and unfolded state. If they had been in equilibrium the apparent melting temperature (T_m) should have been the same regardless of the heating rate (Sanchez-Ruiz 2010).

4.3.3 Comparison of CBP21 wild type and EfCBM33 wild type by adding DTT

In the thermo-stability assay there is a difference in the stability of CBP21 and EfCBM33 (figure 4.16, table 4.2). CBP21 contains disulphide bridges, while EfCBM33 does not; still the latter have an apparent tm 2 °C higher than CBP21 when the heating rate was set to 1°C/min.

This is why both of the enzymes were incubated with DTT a strong reducing agent that reduces disulphide bridges. In this particular assay CBP21 had an apparent melting temperature of 64.1 °C, while EfCBM33 an apparent melting temperature at 70.5 °C (figure4.16, table 4.2). Even though EfCBM33 has no disulphide bridges, the DTT did reduce the stability of both enzymes (6.2 °C for CBP21 and 1.5°C for EfCBM33). The 6 °C reduction in apparent melting temperature caused by DTT in CBP21 indicates that the disulphide bridges contribute significantly to the stabilization of CBP21.
In the studies presented here, it appears that disulfide bridges do not make CBP21 more stable than EfCBM33 but it is apparent that the disulphide bridges do stabilize CBP21 and that the incorporation of more S-S bridges may contribute to an even higher stability. This could also be the case for EfCBM33 as the S-S bridges stabilize the enzymes structure gets more rigid. This has been the case in previous studies (Betz 1993; Lesk 2004).

4.3.4 The addition of metals to the CBP21 solution

Divalent metal ions turned out to be very important for CBP21s enzyme activity (Vaaje-Kolstad et al. 2010) and previously studies with divalent metals have been demonstrated to stabilize proteins at high temperatures, and even making the protein able to unfold irreversibly (Sandberg et al. 2002; Wang et al. 2004). Therefore, excess amount of divalent metal ions were added to the protein solution to see if that would affect thermal-stability (table 4.3). When adding divalent metals to the protein solution, there wasn't any obvious difference in the denaturing process of CBP21 compared to the assays with no additional divalent metals. At least not when adding $MgCl_2$ or $CaCl_2$. But when adding $ZnCl_2$ to the solution, one could see that a small "lump" had disappeared from the thermal stability curve (figure 4.17). The difference was seen at $ZnCl_2$ concentrations at or above 100nM. A dose-response assay with different $ZnCl_2$ concentrations was performed (figure 4.18). The dose response assay shows that $ZnCl_2$ affects the unfolding curve. This "lump", seen without the addition of zinc, could be a premature partial denaturing process that occurs before the denaturing process of the complete protein kicks in, or it could be that the CBP21 enzyme has a three state de-folding process. The dose-response assay revealed that this "lump" disappeared as the $ZnCl_2$ concentration reached 1000nM.

Additional tests where the metals were removed completely with the metal binder EDTA showed that this "lump" became even more obvious (figure 4.17). This indicates that the metals in the binding site of CBP21 has something to do with this "lump", and that $ZnCl_2$ is a metal that can bind the binding site so strong, that the "lump" becomes abolished at high concentrations.

4.3.5 Effect of entropic mutations in CBP21 A130P

Of the four mutants made from CBP21 wt, the mutation A130P was the one that showed increased thermo-stability (figure 4.9), which is the first ever reported mutant of a CBM33 with increased thermal-stability. The apparent melting temperature of A130P increased by 2.2 °C compared to CBP21 wt. The sequence alignment of figure 4.6, including the sequence of two putatively thermo-stable chitin binding proteins, one cellulose binding protein from a thermophilic bacterium and one putative chitin-binding domain from *Enterococcus faecalis* (mesopilic) (figure 4.6) shows that a proline naturally occurs at this position in three out of four sequences, it is also worth noticing that this proline appeared in the same position in EfCBM33, which appeared to have a higher apparent tm than CBP21 wt (see below). In a seed alignment in Pfam which is the basis for the definition of a CBM33 domain, about 50 % of the compared sequences contained the desired proline mutation. One might thus say that the introduction of this proline follows the so-called “consensus” approach (see section 1.16)

The A130P mutation surface located but does not affect the binding surface of CBP21. Although this mutation stabilized the protein, it does not mean that the mutation made the enzyme more active (Robic 2010). In the worst case, the activity may even be reduced. Also, even though the A130P mutation made the enzyme structure more thermo- stable, it does not necessarily mean that the binding site and the catalytic center of CBP21 are stabilized at all. At higher temperatures the binding and catalytic center of the enzyme may be the limiting factors and not the overall structure. Therefore, enzyme activity studies have to be performed before concluding whether a stabilizing mutation such as the A130P mutation in CBP21 is useful (Robic 2010).

4.4 Degradation studies of β-chitin

The activity of CBP21 was measured by looking at the increase in *N*-acetyl-D-glucosamine ($GlcNAc_2$) production as a result of the addition of CBP21 to the degradation of crystalline β-chitin by Chitinase B (figure 4.2). From previous studies (Vaaje-Kolstad 2005) it is known that CBP21 act synergistically with chitinases to enhance the degradation rate of β-chitin. Based on the results from the temperature unfolding studies attempts were made to see the loss of enzyme activity when incubating CBP21 at the melting temperature (about 70 °C). The results were as expected; the enzyme activity was almost completely abolished. Attempts were also made, under the same conditions at 50 °C to see the enzyme activity. These results showed a $GlcNAc_2$ production at 662 µM after 150 minutes, which is about the same as achieved in 2010 by Vaaje-Kolstad et al.

5 Summary and future work

5.1 Summary

Binding experiments done on a UV spectrophotometer with CBP21 wt and β-chitin showed that 16 % of the protein was bound to the substrate after 100 minutes, and that 40 % protein was bound after 480 minutes. This was considerably lower than what Vaaje-Kolstad achieved in 2005 (Vaaje-Kolstad et al. 2005b). This was probably because of the somewhat different substrate that was used, but it could also be that the reproduction of the assay was different compared to the preparation of point zero.

Development of binding assay on a fluorescence spectrophotometer showed that the decline in absorbance of the control with only CBP21 was in many cases higher than the actual enzyme-substrate mixture. This was not due to bleaching of the UV radiation used for excitation.

Refolding tests showed that neither CBP21 wt nor EfCBM33 or the CBP21 mutant Q161A (that was made to prevent aggregation) refolded after cooling down 1 °C/min or at 5 °C/min from 80 °C to 20°C or 0 °C.

CBP21 wild-type unfolded at a higher temperature when the heating rate was at 5 °C/min compared with 1 °C/min. The refolding test and the difference in unfolding with different heating rates show that the thermo-stability of CBP21 wild-type is kinetic.

One of the four mutants made from CBP21 showed increased thermo-stability. This enzyme, A130P, had an apparent melting temperature of 72.5 °C, which was 2.2 °C higher than the CBP21 wild type.

The comparison of thermal-stability between CBP21 and EfCBM33 showed that EfCBM33 has an apparent melting temperature of 72.0 °C while CBP21 wt has an apparent melting temperature at 70.3 °C. Despite the disulphide bridges (S-S), CBP21 is not more thermo-stabile than EfCBM33. The effect of destroying S-S bridges by DTT showed that S-S bridges do stabilize CBP21 at higher temperatures, as the stability of CBP21 decreased with 4 °C.

The divalent metal $ZnCl_2$ did affect the unfolding curve of CBP21 wild type. This effect increased with increased $ZnCl_2$ concentration, when adding $MgCl_2$ or $CaCl_2$ there wasn't any obvious difference in the denaturing process of CBP21 wild-type. In all cases, there were aggregates in the cuvette after heating.

Circular dichroism scans to assay thermo-stability showed that both CBP21 and EfCBM33 have lost most of their structure after heating to 80 °C, reinforcing that the proteins do not refold after heating. Measuring CD signals at 222nm is not the most optimal tool in measuring protein stability in CBP21, but could be interpreted as a loss of helical structure in EfCBM33.

5.2 Future work

Additional studies have to be performed before a conclusion can be made based on the fluorescence binding studies. For example different excitation wavelengths, different buffers and pH could be attempted. Also, the assay should be performed with stirring in the bottom of the cuvette while incubating. This study should also be performed using different protein batches, as it also could be variations in protein stability from one purification of protein to the other.

To get an overview on the effect on stabilizing CBP21 at higher temperatures, degradation studies of β-chitin by CBP21 have to be performed by the CBP21 mutant A130P. This should also be performed on CBP21 wild type and EfCBM33, with various $ZnCl_2$ concentrations and with various divalent metals, to see if their enzyme activity has a dose response for divalent metal concentration. This could be performed on a UHPLC/HPLC to look at the production of oxidized oligosaccharides

(In 2010 Vaaje-Kolstad et al. observed that CBP21 increased the chitinase degradation of β-chitin by adding reductants (such as ascorbic acid and reduced glutate ion). On the basis of this a dose response assay with different concentrations of reductants to look at the dimere production by Chi-B would be interesting. This could also be performed on a UHPLC/HPLC).

To determine if the CBP21 wild-type is able to refold, a thermo-stability assay could be performed by decreasing the temperature to varying degrees below 80 °C. This could be performed on a fluorescence spectrophotometer by measuring decrease and possibly increase in fluorescent signal.

The incorporation of additional disulfide bridges (S-S) to CBP21 to see if this could increase thermal-stability is also a way to go in these studies. It would also be interesting to look at the effect of incorporate S-S bridges to EfCBM33.

6 References

Atkins, E. (1985). CONFORMATIONS IN POLYSACCHARIDES AND COMPLEX CARBOHYDRATES. *Journal of Biosciences*, 8 (1-2): 375-387.

Atkins, P. W. & De Paula, J. (2006). *Atkins' physical chemistry*. Oxford: Oxford University Press. XXX, 1064 s. pp.

Betz, S. F. (1993). DISULFIDE BONDS AND THE STABILITY OF GLOBULAR-PROTEINS. *Protein Science*, 2 (10): 1551-1558.

Boraston, A. B., Bolam, D. N., Gilbert, H. J. & Davies, G. J. (2004). Carbohydrate-binding modules: fine-tuning polysaccharide recognition. *Biochemical Journal*, 382: 769-781.

Brurberg, M. B., Nes, I. F. & Eijsink, V. G. H. (1996). Comparative studies of chitinases A and B from Serratia marcescens. *Microbiology-Uk*, 142: 1581-1589.

Burtis, C. A., Ashwood, E. R., Border, B. G. & Tietz, N. W. (2001). *Tietz fundamentals of clinical chemistry*. Philadelphia: Saunders. XXV, 1091 s. pp.

Bøhle, L. A., Gåseidnes, S., Westereng, B., Dalhus, B., Bjørås, M., Mathiesen, G., Eijsink, V. G. H. & Vaaje-Kolstad, G. (2011). *Structural and functional analysis of the Enterococcus faecalis CBM33 oxidohydrolase*. Ås: Department of Chemistry, Biotechnology and Food Science, Norwegian University of Life Sciences. 2 pp. Unpublished manuscript.

Chan, H. K., AuYeung, K. L. & Gonda, I. (1996). Effects of additives on heat denaturation of rhDNase in solutions. *Pharmaceutical Research*, 13 (5): 756-761.

Chen, J. M. & Stites, W. E. (2001). Packing is a key selection factor in the evolution of protein hydrophobic cores. *Biochemistry*, 40 (50): 15280-15289.

Cooper, G. M. & Hausman, R. E. (2007). *The cell: a molecular approach*. Washington: ASM Press/Sinauer Associates. XIX, 820 s. pp.

Degré, M. (2000). *Medisinsk mikrobiologi*. Oslo: Gyldendal akademisk. 739 s. pp.

DeLano, W. L. (2002). *The PyMOL Molecular Graphics System*. San Carlos: DeLano Scientific. Available at: http://www.pymol.org.

Dionisi, H. M., Alvarez, C. V. & Viale, A. M. (1999). Alkali metal ions protect mitochondrial rhodanese against thermal inactivation. *Archives of Biochemistry and Biophysics*, 361 (2): 202-206.

Eijsink, V. G., Vaaje-Kolstad, G., Varum, K. M. & Horn, S. J. (2008). Towards new enzymes for biofuels: lessons from chitinase research. *Trends Biotechnol*, 26 (5): 228-35.

Eijsink, V. G. H., Bjork, A., Gaseidnes, S., Sirevag, R., Synstad, B., van den Burg, B. & Vriend, G. (2004). Rational engineering of enzyme stability. *Journal of Biotechnology*, 113 (1-3): 105-120.

Forsberg, Z., Vaaje-Kolstad, G., Westereng, B., Bunaes, A. C., Stenstrom, Y., Mackenzie, A., Sorlie, M., Horn, S. J. & Eijsink, V. G. (2011). Cleavage of cellulose by a CBM33 protein. *Protein Sci*.

Gooday, G. W. (1990). THE ECOLOGY OF CHITIN DEGRADATION. *Advances in Microbial Ecology*, 11: 387-430.

Harris, P. V., Welner, D., McFarland, K. C., Re, E., Poulsen, J. C. N., Brown, K., Salbo, R., Ding, H. S., Vlasenko, E., Merino, S., et al. (2010). Stimulation of Lignocellulosic Biomass Hydrolysis by Proteins of Glycoside Hydrolase Family 61: Structure and Function of a Large, Enigmatic Family. *Biochemistry*, 49 (15): 3305-3316.

Hart, H., Crane, L. E., Hart, D. J. & Hadad, C. M. (2007). *Organic chemistry: a short course*. Boston: Houghton Mifflin. XXIV, 577 s. pp.

Henrissat, B. & Romeu, A. (1995). FAMILIES, SUPERFAMILIES AND SUBFAMILIES OF GLYCOSYL HYDROLASES. *Biochemical Journal*, 311: 350-351.

Henrissat, B. & Davies, G. (1997). Structural and sequence-based classification of glycoside hydrolases. *Current Opinion in Structural Biology*, 7 (5): 637-644.

Henrissat, B., Coutinho, P. O., Rancurel, C. & Lombard, V. (1998). *CAZy Carbohydrate-Active Enzymes*. Marseille cedex 9: Glycogenomics group at Architecture et Fonction des Macromolécules Biologiques (AFMB). Available at: http://www.cazy.org (accessed: 17.06.).

Horn, S. J., Sikorski, P., Cederkvist, J. B., Vaaje-Kolstad, G., Sorlie, M., Synstad, B., Vriend, G., Varum, K. M. & Eijsink, V. G. (2006a). Costs and benefits of processivity in enzymatic degradation of recalcitrant polysaccharides. *Proc Natl Acad Sci U S A*, 103 (48): 18089-94.

Horn, S. J., Sorbotten, A., Synstad, B., Sikorski, P., Sorlie, M., Varum, K. M. & Eijsink, V. G. H. (2006b). Endo/exo mechanism and processivity of family 18 chitinases produced by Serratia marcescens. *Febs Journal*, 273 (3): 491-503.

Hrmova, M. & Fincher, G. B. (2001). Structure-function relationships of beta-D-glucan endo- and exohydrolases from higher plants. *Plant Molecular Biology*, 47 (1-2): 73-91.

Janecek, S. (1993). SEQUENCE SIMILARITIES IN (ALPHA-BETA)8-BARREL ENZYMES REVEALED BY CSERVED REGIONS OF ALPHA-AMYLASE. *Febs Letters*, 316 (1): 23-26.

Jiskoot, W. & Crommelin, D. J. A. (2005). *Methods for structural analysis of protein pharmaceuticals / Wim Jiskoot, Daan J.A. Crommelin*. Biotechnology: pharmaceutical aspects. New York: AAPS Press.

Kozlowski, H., Janicka-Klos, A., Stanczak, P., Valensin, D., Valensin, G. & Kulon, K. (2008). Specificity in the Cu2+ interactions with prion protein fragments and related His-rich peptides from mammals to fishes. *Coordination Chemistry Reviews*, 252 (10-11): 1069-1078.

Kristjansson, M. M. & Kinsella, J. E. (1991). Protein and enzyme stability: structural, thermodynamic, and experimental aspects. *Adv Food Nutr Res*, 35: 237-316.

Larkin, M. A., Blackshields, G., Brown, N. P., Chenna, R., McGettigan, P. A., McWilliam, H., Valentin, F., Wallace, I. M., Wilm, A., Lopez, R., et al. (2007). Clustal W and Clustal X version 2.0. *Bioinformatics*, 23 (21): 2947-2948.

Lehmann, M., Kostrewa, D., Wyss, M., Brugger, R., D'Arcy, A., Pasamontes, L. & van Loon, A. (2000). From DNA sequence to improved functionality: using protein sequence comparisons to rapidly design a thermostable consensus phytase. *Protein Engineering*, 13 (1): 49-57.

Lesk, A. M. (2004). *Introduction to protein science: architecture, function, and genomics*. Oxford: Oxford University Press. XVI, 310 s. pp.

Manoil, C. & Beckwith, J. (1986). A GENETIC APPROACH TO ANALYZING MEMBRANE-PROTEIN TOPOLOGY. *Science*, 233 (4771): 1403-1408.

Matthews, B. W., Nicholson, H. & Becktel, W. J. (1987). ENHANCED PROTEIN THERMOSTABILITY FROM SITE-DIRECTED MUTATIONS THAT DECREASE THE ENTROPY OF UNFOLDING. *Proceedings of the National Academy of Sciences of the United States of America*, 84 (19): 6663-6667.

McMurry, J., Castellion, M. E. & Ballantine, D. S. (2007). *Fundamentals of general, organic, and biological chemistry*. Upper Saddle River, N.J.: Pearson Education International. XXVII, 889 s. pp.

Miyazaki, J., Nakaya, S., Suzuki, T., Tamakoshi, M., Oshima, T. & Yamagishi, A. (2001). Ancestral residues stabilizing 3-isopropylmalate dehydrogenase of an extreme thermophile: Experimental evidence supporting the thermophilic common ancestor hypothesis. *Journal of Biochemistry*, 129 (5): 777-782.

Pace, C. N. (1990). MEASURING AND INCREASING PROTEIN STABILITY. *Trends in Biotechnology*, 8 (4): 93-98.

Page, M. J. & Di Cera, E. (2006). Role of Na+ and K+ in enzyme function. *Physiological Reviews*, 86 (4): 1049-1092.

Proctor, M. R., Taylor, E. J., Nurizzo, D., Turkenburg, J. P., Lloyd, R. M., Vardakou, M., Davies, G. J. & Gilbert, H. J. (2005). Tailored catalysts for plant cell-wall degradation: Redesigning the exo/endo preference of Cellvibrio japonicus arabinanase 43A. *Proceedings of the National Academy of Sciences of the United States of America*, 102 (8): 2697-2702.

Righetti, P. G. & Verzola, B. (2001). Folding/unfolding/refolding of proteins: Present methodologies in comparison with capillary zone electrophoresis. *Electrophoresis*, 22 (12): 2359-2374.

Rinaudo, M. (2006). Chitin and chitosan: Properties and applications. *Progress in Polymer Science*, 31 (7): 603-632.

Rouvinen, J., Bergfors, T., Teeri, T., Knowles, J. K. C. & Jones, T. A. (1990). 3-DIMENSIONAL STRUCTURE OF CELLOBIOHYDROLASE-II FROM TRICHODERMA-REESEI. *Science*, 249 (4967): 380-386.

Sandberg, A., Leckner, J., Shi, Y., Schwarz, F. P. & Karlsson, B. G. (2002). Effects of metal ligation and oxygen on the reversibility of the thermal denaturation of Pseudomonas aeruginosa azurin. *Biochemistry*, 41 (3): 1060-1069.

Sterner, R. & Hocker, B. (2005). Catalytic versatility, stability, and evolution of the (betaalpha)8-barrel enzyme fold. *Chem Rev*, 105 (11): 4038-55.

Suzuki, K., Suzuki, M., Taiyoji, M., Nikaidou, N. & Watanabe, T. (1998). Chitin binding protein (CBP21) in the culture supernatant of Serratia marcescens 2170. *Bioscience Biotechnology and Biochemistry*, 62 (1): 128-135.

Synstad, B., Gaseidnes, S., van Aalten, D. M. F., Vriend, G., Nielsen, J. E. & Eijsink, V. G. H. (2004). Mutational and computational analysis of the role of conserved residues in the active site of a family 18 chitinase. *European Journal of Biochemistry*, 271 (2): 253-262.

Tews, I., vanScheltinga, A. C. T., Perrakis, A., Wilson, K. S. & Dijkstra, B. W. (1997). Substrate-assisted catalysis unifies two families of chitinolytic enzymes. *Journal of the American Chemical Society*, 119 (34): 7954-7959.

Tortora, G. J., Case, C. L. & Funke, B. R. (2007). *Microbiology: an introduction*. San Francisco: Pearson Benjamin Cummings. XXVI, 958 s. pp.

van den Burg, B. & Eijsink, V. G. H. (2002). Selection of mutations for increased protein stability. *Current Opinion in Biotechnology*, 13 (4): 333-337.

van Aalten, D. M. F., Synstad, B., Brurberg, M. B., Hough, E., Riise, B. W., Eijsink, V. G. H. & Wierenga, R. K. (2000). Structure of a two-domain chitotriosidase from Serratia marcescens at 1.9-angstrom resolution. *Proceedings of the National Academy of Sciences of the United States of America*, 97 (11): 5842-5847.

van Aalten, D. M. F., Komander, D., Synstad, B., Gaseidnes, S., Peter, M. G. & Eijsink, V. G. H. (2001). Structural insights into the catalytic mechanism of a family 18 exo-chitinase. *Proceedings of the National Academy of Sciences of the United States of America*, 98 (16): 8979-8984.

Vuong, T. V. & Wilson, D. B. (2010). Glycoside Hydrolases: Catalytic Base/Nucleophile Diversity. *Biotechnology and Bioengineering*, 107 (2): 195-205.

Vaaje-Kolstad, G. (2005). *The chitinolytic machinery of Serratia marcescens: the catalytic mechanism of chitinase B and the function of the chitin-binding protein, CBP21*. Ås: Universitetet, UMB. 1 b. (flere pag.) pp.

Vaaje-Kolstad, G., Horn, S. J., van Aalten, D. M., Synstad, B. & Eijsink, V. G. (2005a). The non-catalytic chitin-binding protein CBP21 from Serratia marcescens is essential for chitin degradation. *J Biol Chem*, 280 (31): 28492-7.

Vaaje-Kolstad, G., Houston, D. R., Riemen, A. H., Eijsink, V. G. & van Aalten, D. M. (2005b). Crystal structure and binding properties of the Serratia marcescens chitin-binding protein CBP21. *J Biol Chem*, 280 (12): 11313-9.

Vaaje-Kolstad, G., Westereng, B., Horn, S. J., Liu, Z. L., Zhai, H., Sorlie, M. & Eijsink, V. G. H. (2010). An Oxidative Enzyme Boosting the Enzymatic Conversion of Recalcitrant Polysaccharides. *Science*, 330 (6001): 219-222.

Vaaje-Kolstad, G., Bøhle, L. A., Dalhus, B., Bjørås, M., Mathiesen, G. & Eijsink, V. G. H. (2011). *THE CHITINOLYTIC MACHINERY OF ENTEROCOCCUS FAECALIS V583 INCLUDES AN ENZYMATICALLY ACTIVE CBM33 THAT PROMOTES POLYSACCHARIDE DEGRADATION USING A NOVEL OXIDATIVE MECHANISM*. Ås: Department of Chemistry, Biotechnology and Food Science, Norwegian University of Life Sciences, P. O. Box 5003, N-1432 Ås, Norway

Institute of Medical Microbiology, Oslo University Hospital, N-0027 Oslo, Norway. Unpublished manuscript.

Wang, S. C., Dias, A. V., Bloom, S. L. & Zamble, D. B. (2004). Selectivity of metal binding and metal-induced stability of Escherichia coli NikR. *Biochemistry*, 43 (31): 10018-10028.

Waters. (1995). *ACQUITY UPLC BEH AMIDE COLUMS*. In RESERVED, W. A. R. (ed.). 34 Maple Street, Milford, Massachusetts, 01757, USA: Waters Corporation. Available at: http://www.waters.com/webassets/cms/library/docs/720003122en.pdf?ev=10118801&locale=en_US.

Watson, J. D. (2008). *Molecular biology of the gene*. Cold Spring Harbor, N.Y.: CSHL Press. XXXII, 841 s. pp.

Wei, W. (1999). Instability, stabilization, and formulation of liquid protein pharmaceuticals. *International Journal of Pharmaceutics*, 185 (2): 129-188.

Withers, S. (2010). *Carbohydrate-active enzymes*. In Williams, S. (ed.): CAZypedia. Available at: http://www.cazypedia.org/index.php/Carbohydrate-active_enzymes (accessed: 17 January).

Withers, S. & Williams, S. (2011). *Glycoside hydrolases*: cazypedia. Available at: http://www.cazypedia.org/index.php/Glycoside_hydrolases.

Woody, R. W. (1995). CIRCULAR-DICHROISM. *Biochemical Spectroscopy*, 246: 34-71.

Wren, S. A. C. & Tchelitcheff, P. (2006). Use of ultra-performance liquid chromatography in pharmaceutical development. *Journal of Chromatography A*, 1119 (1-2): 140-146.

Zor, T. & Seliger, Z. (1996). Linearization of the bradford protein assay increases its sensitivity: Theoretical and experimental studies. *Analytical Biochemistry*, 236 (2): 302-308.

Aam, B. B., Heggset, E. B., Norberg, A. L., Sorlie, M., Varum, K. M. & Eijsink, V. G. H. (2010). Production of Chitooligosaccharides and Their Potential Applications in Medicine. *Marine Drugs*, 8 (5): 1482-1517.